An improved perspective in the spatial representation of soil moisture: potential added value of SMOS disaggregated 1 km resolution "all weather" product

Samiro Khodayar[1], Amparo Coll[2], Ernesto Lopez-Baeza[2]

[1] Institute of Meteorology and Climate Research (IMK-TRO), Karlsruhe Institute of Technology (KIT), Karlsruhe, Germany

[2] University of Valencia, Spain. Earth Physics and Thermodynamics Department. Climatology from Satellites Group

Submitted to HESS

* Corresponding author. E-mail address: samiro.khodayar@kit.edu (S. Khodayar)

Institute for Meteorology and Climate Research, Karlsruhe Institute of Technology (KIT), Postfach 3640, 76021 Karlsruhe, Germany

Abstract

This study uses the synergy of multiresolution soil moisture (SM) satellite estimates from the Soil Moisture Ocean Salinity (SMOS) mission, a dense network of ground-based SM measurements, and a Soil Vegetation Atmosphere Transfer (SVAT) model, SURFEX (Externalized Surface) – module ISBA (Interactions between Soil-Biosphere-Atmosphere), to examine the benefits of the SMOS L4 version 3.0 or "all weather" high resolution soil moisture disaggregated product (~ 1 km, $SMOS\_L4^{3.0}$). The added value compared to SMOS-L3 (~ 25 km) and L2 (~15 km) is investigated. In situ SM observations over the Valencia Anchor Station (VAS; SMOS Calibration/Validation (Cal/Val) site in Europe) are used for comparison. The SURFEX(ISBA) model is used to simulate point-scale surface SM (SSM) and, in combination with high-quality atmospheric information data, namely ECMWF and the SAFRAN meteorological analysis system, to obtain a representative SSM mapping over the VAS. The sensitivity to realistic initialization with $SMOS\_L4^{3.0}$ to simulate the spatial and temporal distribution of SSM is assessed. Results demonstrate: (a) all SMOS products correctly capture the temporal patterns, but, the spatial patterns are not accurately reproduced by the coarser resolutions probably in relation to the contrast with point-scale in situ measurements. (b) The potential of $SMOS\text{-}L4^{3.0}$ product is pointed out to adequately characterize SM spatio-temporal variability reflecting patterns consistent with intensive point scale SSM samples on a daily time scale. The restricted temporal availability of this product dictated by the revisit period of the SMOS satellite compromises the averaged SSM representation for longer periods than a day. (c) A seasonal analysis points out improved consistency during December-January-February and September-October-November in contrast to significantly worse correlations in March-April-May (in relation to the growing vegetation) and June-July-August (in relation to low SSM values < 0.1 m^3/m^3 and low spatial variability). (d) The combined use of the SURFEX(ISBA) SVAT model with the SAFRAN

system, initialized with SMOS-L4$^{3.0}$ 1 km disaggregated data is proven to be a suitable tool to produce regional SM maps with high accuracy which could be used as initial conditions for model simulations, flood forecasting, crop monitoring and crop development strategies, among others.

Key Words: soil moisture, SMOS 1-km disaggregated product, SURFEX, Valencia Anchor Station, realistic initialization, SAFRAN

1. Introduction

Reliability of climate and hydrological models is constrained by associated uncertainties, such as input parameters. Among them, soil moisture is a variable of pivotal importance controlling the exchanges of water and energy at the surface/atmosphere interface (Entekhabi et al., 1996). Thus, it is a highly relevant variable for climate, hydrology, meteorology and related disciplines (e.g. Seneviratne et al. 2010).

Soil moisture is greatly variable spatially, temporally and across scales. The spatial heterogeneity of soil, vegetation, topography, land cover, rainfall and evapotranspiration are accounted responsible (Western et al., 2002; Bosh et al., 2007; Rosenbum et al. 2012).

The response of soil moisture to precipitation changes largely depends on soils water capacity and climatic zones. Particularly, in dry climates such as the Iberian Peninsula (IP), soil moisture quickly reacts to changes in precipitation (Li and Rodell 2013). Precipitation variability and mean are positively correlated, thus, an increase in precipitation yields wetter soils, which in turn results in higher spatial variability of soil moisture. An adequate representation of the high spatio-temporal variability of soil moisture is needed to improve climate and hydrological modelling (Koster et al., 2004; Seneviratne et al., 2006; Brocca et al., 2010). Its impact has been seen on time scales from hours to years (e.g., ~ 20 km scale: Taylor and Lebel, 1998; droughts: Schubert et al., 2004; decadal drying of the Sahel: Walker and Rowntree, 1977; hot extremes: Seneviratne et al., 2006b; Hirschi et al., 2011; decadal simulations: Khodayar et al., 2014). To obtain an appropriate representation of this variable, especially at high-resolution, is not an easy task mainly because of its high variability. Methods for the estimation of soil moisture can be divided in three main categories, (i) measurement of soil moisture in the field, (ii) estimation via simulation models, and (iii) measurement using remote sensing. In general, in situ measurements are far from global (e.g., Robock et al. 2000), and model simulations present important biases. Therefore, we have to rely on space-borne sensors to provide such measurements, but until recent times no dedicated, long-term, moisture space mission was attempted (Kerr, 2007).

Nowadays, by means of remote sensing technology surface soil moisture is available at global scale (Wigneron et al., 2003). The best estimations result from microwave remote sensing at low frequencies (e.g. Kerr, 2007; Jones et al., 2011) and several global soil moisture products have been produced, such as the European Space Agency's Climate Change Initiative (ESA CCI, Liu et al. 2011; Wagner et al. 2012) soil moisture products, the soil Moisture Active Passive (SMAP; Entekhabi et al. 2010), the Advanced Microwave Scanning Radiometer-EOS (AMSR-E; Owe et al. 2008), the advanced scatterometer (ASCAT; Naeimi et al. 2009) and the Soil Moisture and Ocean Salinity (SMOS; Kerr et al., 2001) .

The SMOS mission is the first space-borne passive L-band microwave (1.4 GHz) radiometer measuring at low frequency soil moisture over continental surfaces as well as ocean salinity (Kerr et al., 2001, 2010). SMOS delivers global surface soil moisture measurements (~ 0-5 cm depth) at 0600 a.m. and 0600 p.m. LT (local time) in less than 3-days revisit at a spatial resolution of ~ 44 km. The benchmark of the mission is to reach accuracy better than 0.04 m^3/m^3 for the provided global maps of soil moisture (Kerr et al., 2001).

SMOS data is not exempt of biases. Validating remote sensing-derived soil moisture products is difficult, e.g. due to scale differences between the satellite footprints and the point measurements on the ground (Cosh et al., 2004). However, in the last years a huge effort has been made to validate the SMOS algorithm and its associated products. With this purpose, in situ measurements across a range of climate regions were used assessing the reliability and accuracy of these products using independent measurements (Delwart et al., 2008; Juglea et al., 2010; Bircher et al., 2012; Dente et al., 2012; Gherboudj et al., 2012; Sánchez et al., 2012; Wigneron et al., 2012). The strategy adapted by the European Space Agency (ESA) was to develop specific land product validation activities over well-equipped monitoring sites. An example for this is the Valencia Anchor Station (VAS; Lopez-Baeza et al., 2005a) in eastern Spain, which was chosen as one of the two main test sites in Europe for the SMOS Calibration/Validation (Cal/Val) activities. The validation sites were chosen to be slightly larger than the actual pixel (3dB footprint), thus, VAS covers a 50x50 km^2 area. Within this area, a limited number of ground stations were installed relying on spatialized soil moisture information using the SVAT (Soil Vegetation Atmospheric Transfer) SURFEX (Externalized Surface) model. Worldwide validation results reveal a coefficient of determination (R^2) of about 0.49 when comparing the ~5 cm in situ soil moisture averages and the SMOS soil moisture level 2 (SMOS-L2 ~ 15 km). For example, validation results by Bircher et al. (2012) in Western Denmark show R^2 of 0.49-0.67 (SMOS retrieved initial soil moisture) and 0.97 (SMOS retrieved initial temperature). Besides, a significant under-/over-representation of the network data (biases of – 0.092-0.057 m^3/m^3) is also found. Over the Maqu (China) and the Twente (The Netherlands) regions, the validation analysis resulted in R^2 of 0.55 and 0.51, respectively, for the ascending pass observations, and of 0.24 and 0.41, for the descending pass observations. Furthermore, Dente et al. (2012) pointed out a systematic SMOS soil moisture (ascending pass observations) dry bias of about 0.13 m^3/m^3 for the Maqu region and 0.17 m^3/m^3 for the Twente region. Validation of the SMOS level 3 product (SMOS-L3 ~ 35 km) shows that the general dry bias in SMOS-L2 is also present in SMOS-L3 SM. This bias is markedly present in the ascending products and shorter time series as described in Sanchez et al. (2012) and Gonzalez-Zamora et al. (2015). In this case, the presence of dense vegetation is seen to increase RMSE scores, whereas in low vegetated areas a lower dry bias is found (Louvet et al. 2015).

Since the launch of the SMOS satellite, the processing prototypes of the SMOS L2 soil moisture have evolved, and their quality has improved. Furthermore, efforts have been made to cover the need of a reliable product with finer resolution for hydrological and climatic studies where the spatial variability of soil moisture plays a crucial role, e.g. in the estimation of land surface fluxes (evapotranspiration (ET) and runoff). Piles et al. (2011) presented a downscaling approach to optimally combine SMOS´ soil moisture estimates with MODIS (Moderate Resolution Imaging Spectroradiometer) visible/infrared (VIS/IR) satellite data into 1 km soil moisture maps over the IP without significant degradation of the root mean square error (RMSE). This product has been evaluated using the REMEDHUS (REd de MEDicion de la HUmedad del Suelo) soil moisture network in the semi-arid area of the Duero basin, Zamora, Spain (Piles et al. 2014). Results show that downscaling maintains temporal correlation and root mean squared differences with ground-based measurements, hence, capturing the soil moisture dynamics. Complementary studies after Piles et al. (2011) have produced similar downscaled high-resolution SMOS-L4 soil moisture products (e.g. Malbéteau et al (2018); Djamai et al (2016)). Being similar, however, the algorithms originating them are totally different from those of SMOS-L4 used in this study. Whereas SMOS-L4 products in this study proceed from the original SMOS-L2 (15 km resolution soil moisture) disaggregated by 1-km MODIS LST and NDVI, Malbéteauet al (2018) and Djamaiet al (2016) products proceed from the original SMOS-L1 (15 km resolution brightness temperature).

A big limitation for the downscaling approach used in Piles et al. (2011) is the lack of information in cloudy conditions of the hereafter named SMOS_L4$^{2.0}$, which significantly limits the availability and usefulness of this product. In this study, we examine a new version of the SMOS_L4 product, the SMOS Level 4 3.0 "all weather" disaggregated ~ 1 km SM (SMOS_L4$^{3.0}$), which was developed and has been recently made available by SMOS-BEC (Barcelona Expertise Centre).In this advanced high-resolution soil moisture product the limitation on clouds is modulated by the use of ERA-Interim LST data, thus providing soil moisture measurements independently of the cloud conditions.

Contrary toSMOS-L3 and -L2 products, which have been extensively validated as described above and used for assimilation purposes in models (e.g. De Lannoy et al. 2016; Leroux et al. 2016), few studies deal with the disaggregated 1 km SMOS-$L4^{0.2}$ and SMOS-$L4^{0.3}$ products (mostly in relation to wildfire activity) and validation efforts have concentrated only on the REMEDHUS soil moisture network in Zamora (north-western Spain; e.g. Piles et al. 2014). The objective of this paper is to provide information about the advantages and drawbacks and the added value of the disaggregated 1 km SMOS-$L4^{3.0}$ “all weather” soil moisture product with respect to coarser resolution products. The proposed investigation covers a one year period (a complete hydrological cycle) and focuses on the semi-arid VAS area (eastern Spain) and the IP where water availability and fire risk are big environmental issues, thus, knowledge of soil moisture conditions is of pivotal importance. Furthermore, as spring time soil moisture anomalies over the IP are believed to be a pre-cursor to droughts and heat waves in Europa (Vautard et al. 2007; Zampieri et al. 2009), accurate monitoring and prediction of surface states in this region may be key for improvements in seasonal forecasting systems.

The following objectives are then pursued: (a) Examination of soil moisture temporal and spatial distribution with SMOS-derived soil moisture products over the investigation domain using a multi-resolution approach: L3 (~ 25 km), L2 (~15 km), and $L4^{3.0}$ (~ 1 km), (b) Validation with the in situ soil moisture measurements’ network (VAS) to estimate the reliability of the SMOS SM products, and (c) Evaluation of the impact of realistic SM initialization using SMOS-$L4^{3.0}$ on point-scale and regional SURFEX(ISBA) model simulations over the VAS area.

This investigation is structured as follows, in Section 2, the study area and the data sets are presented including the in situ network measurements, the SMOS data products, and the SURFEX(ISBA) model and related atmospheric forcings used. Section 3 summarizes the methodology applied. The results are discussed in Section 4. Finally, conclusions are drawn in Section 5.

2. Study area and data set

2.1 Investigation domain and in situ measurements over the VAS

The main investigation areas in this study are the Iberian Peninsula and the Valencia Anchor Station (VAS) site located in eastern Spain (39.69°-39.22° N,-1.7°-(-1.11°) W). The VAS site covering approximately a 50x50 km^2 area was established in December 2001 by the University of Valencia as a Calibration/Validation (Cal/Val) site for different low-resolution Earth Observation data products (Bolle et al., 2006). The extension and homogeneity of the area as well as the mostly flat conditions (slopes lower than 2%) make it an ideal reference site. Nevertheless, the small variations in the area, 750 to 950 m, influence the climate of the region, which oscillates between semiarid to dry-sub-humid. Most of the area is dedicated to vineyards (65%), followed by trees, shrubs, forest and industrial and urban cover types. Mostly bare soil conditions are observed beside the vineyard growing season (March/April to September/October). Mean temperatures in the region are between 12°C and 14°C with annual mean precipitation about 450 mm, with maximums in spring and autumn. Within the VAS, a network consisting of eight ThetaProbe ML2x soil moisture stations was deployed by the Climatology from Satellites Group from the Earth Physics and Thermodynamics Department at the University of Valencia. The eight in situ stations are distributed over a 10x10 km^2 area (Figure 1), according to land use, soil type, and other environmental conditions. Details about the characteristics of each station are summarized in Table 1. Soil moisture measurements every 10 min, mostly from 2006, were carried out for the top first 5 cm. More details about the VAS characteristics and soil moisture measurements could be found in Juglea et al. (2010). Precipitation measurements over the IP and the VAS are from the AEMET (Agencia Estatal de Meteorología; Spanish Weather Service) network. Measurements every 10 min are available.

2.2 The SMOS surface soil moisture products

ESA's derived SMOS Soil Moisture Level 2 (SMOS-L2) data product, ~ 15 km, contains the retrieved soil moisture and optical thickness and complementary parameters such as atmospheric water vapour content, radio frequency interferences and other flags. The SMOS-L2 algorithms have been refined since the launch of SMOS, resulting in more precise SM retrievals (ARRAY, 2014). The Level 3 SM product, SMOS-L3, was obtained from the operational CATDS archive. This is a daily product that contains filtered data. The best estimation of SM is selected for each node when several multi-orbit retrievals are available for a given day. A detection of particular events is also performed in order to flag the data. The processing of the data separates morning and afternoon orbits. The aggregated products are generated from this fundamental product. The Level 4 SM, SMOS-L4 2.0 data (SMOS-$L4^{2.0}$), with 1 km spatial resolution is provided by BEC and covers the IP, Balearic Islands, Portugal, South of France, and North of Morocco (latitudes 34°– 45° N and longitudes 10° W – 5° E). A downscaling method that combines highly accurate, but low-resolution SMOS radiometric information (SMOS-L2 data) with high-resolution (brightness temperature measurements), but low sensitivity, visible-to-infrared imagery (NDVI (Normalized Difference vegetation Index) and LST (Land Surface Temperature) from Aqua MODIS) to SSM across spatial scales is used to derive the SMOS-$L4^{2.0}$ data (Piles et al 2010). The impact of using different vegetation indices from MODIS with higher spatial and temporal resolution in the downscaling method was explored in Sanchez-Ruiz et al. (2014), showing that the use of more frequent and higher spatial-resolution vegetation information lead to improved SM estimates. The latest SMOS-L4 product is the version 3.0 or "all weather" (SMOS-$L4^{3.0}$), which is the product used and examined in this study. The downscaling approach is based on Piles et al. (2014) and Sanchez-Ruiz et al. (2014), with the novelty of introducing ERA-Interim LST data in the MODIS LST/NDVI scape, thus providing soil moisture measurements independently of the cloud conditions. ERA-Interim provides a resolution of about 0.125°, whereas MODIS is a ~ 1 km product. The evaluation of the SMOS-L4 2.0 and 3.0 products support the use of the "all weather" version, since it does not depend on cloud cover and the accuracy of the estimates with respect to in-situ data is improved or preserved (Piles et al. (2015), SMOS-BEC Team (2016)).

In this study, the SMOS-L2 V5.51 data coming from a L1C input product (obtained from MIRAS measurements), the SMOS-L3 V2.72 and the SMOS-L4 V3.0 are employed.

2.3 The SURFEX(ISBA) SVAT model

The SVAT model SURFEX (Externalized Surface, Le Moigne et al. 2009) – module ISBA (Interactions between Soil-Biosphere-Atmosphere, Noilhan and Planton 1989) is used to generate point-scale and spatially distributed SM spatial at 1 km grid spacing and temporal fields from initial conditions and atmospheric forcing. SURFEX(ISBA) was developed at the National Center for Metorological Research (CNRM), at Météo France, and it has been widely validated over vegetated and bare surfaces (e.g. Calvet et al. 1998). The ISBA scheme uses the Clapp and Hornberger (1978) soil water model and Darcy's law for the estimation of the diffusion of water in the soil, and allows 12 land use and related vegetation parameterization types. Crops are considered for the VAS area since mainly vineyards, almond and olive trees and shrubs compose the region.

The surface characteristics are considered in the SVAT input, roughness and the fraction of vegetation are adopted from ECOCLIMAP (Masson et al. 2003), topography is obtained from GTOPO (GTOPO30 Documentation) and soil types are defined using FAO (FAO, 2014).

To obtain an accurate simulation of soil moisture in the study area, the model was originally calibrated by Juglea et al. (2010) to be applied over the entire site for any season/year. Particularly relevant for this study is the specific definition of the soil hydraulic parameters which they made for the VAS area, since most of the hydrological parameters are site dependent and not available from SMOS observations. A new set of empirical equations as a function of the percentages of sand and clay was defined using Cosby et al. (1984) and Boone et al. (1999). New definitions and recommendations by Juglea et al. (2010) for the VAS area were adopted in this investigation.

Atmospheric forcing information: ECMWF and SAFRAN

High quality atmospheric forcing is needed to carry out accurate simulations. To run the SURFEX(ISBA) model, the following atmospheric forcing data are needed: air temperature and humidity at screen level, atmospheric pressure, precipitation, wind speed and direction and solar and atmospheric radiation. Three different sets of atmospheric forcing information are used in this study as input forcing for the SURFEX(ISBA) simulations; (a) SURFEX-OBS: meteorological data from 3 fully equipped stations in the OBS area, MELBEX-I, MELBEX-II and VAS, (b) SURFEX-ECMWF: ECMWF (European Centre for Medium-Range Weather Forecast) data, and (c) SURFEX-SAFRAN: information from the SAFRAN (Système d’Analyse Fournissant des Renseignements Atmosphériques à la Neige) meteorological analysis system (Durand et al. 1999; Quintana-Seguí et al. 2008; Vidal et al. 2010).

Precipitation, air temperature, surface pressure, air specific humidity, wind speed and direction, downward longwave radiation, diffuse shortwave radiation, downward direct shortwave radiation, snowfall rate and CO_2 concentration are used as input data from the meteorological stations aforementioned in the OBS area. A temporal resolution of 10 min is available. From ECMWF, dew point and temperature at 2 m, pressure, precipitation and wind components, are used as forcing data, with a 6 h temporal resolution and 0.125°x0.125° spatial resolution. Precipitation, air temperature, surface pressure, air specific humidity, wind speed and downward shortwave and longwave radiation from SAFRAN are used as input information with a spatial resolution of 8x8 km^2 and an hourly temporal resolution. In this last case, we have an optimal spatial and temporal distribution of the atmospheric forcing over the VAS area (~ 50x50 km^2) and a rare to find complete database to force the land surface model. More details about the SAFRAN system and its validation in north-eastern Spain could be found in Quintana-Seguí et al. (2016).

3. Analysis methodology

In order to investigate the characteristics and potential added values of fine-scale SMOS-derived soil moisture, the spatial variability, the temporal evolution as well as the probability distribution is investigated. With this purpose, SMOS-derived soil moisture products at different spatial resolutions, in situ measurements and model simulations are jointly evaluated.

The spatial distribution and temporal evolution of precipitation and SMOS-derived soil moisture over the IP and the VAS area are assessed for the time period from December 2011 to December 2012 considering also hydrological seasons (DJF: December-January-February, MAM: March-April-May, JJA: June-July-August, SON: September-October-November). Special attention is paid to the autumn season since in this period the western Mediterranean is characterized by a large thermal gradient between the atmosphere and the sea (Duffourg and Ducrocq, 2011, 2013) resulting in intense precipitation extremes (Raveh-Rubin and Wernli 2015). Furthermore, during 2012, the Hydrological Cycle in the Mediterranean Experiment (HyMeX; Dobrinski et al. 2014) took place in the Western Mediterranean with the IP and particularly the Valencia region as target areas. During the SON period of 2012, the Special Observation Period (SOP1; Ducrocq et al. 2014) with intensive experimental deployment over the area took place. This provides us with valuable information about the environmental conditions as well as the occurrence of precipitation events in the investigation area. Particularly, precipitation in the IP during the autumn (SON) period of 2012 was above average (Khodayar et al. 2015). It was also the hydrological season in which higher variability in the soil moisture was observed as a result of the precipitation distribution. Two unique events, at the end of September (27-29) affecting south and eastern Spain and at the end of November (19-20) affecting the Ebro valley (Jansà et al. 2014), largely determined the positive anomaly in precipitation and soil moisture in this period.

SMOS-L3 (~ 25 km), SMOS-L2 (~ 15 km), and SMOS-$L4^{3.0}$ (~ 1km) are used for the evaluation of soil moisture distribution at different grid spacing. Piles et al. (2014) pointed out that differences may exist between SMOS-L3–L2 and the 1 km disaggregated soil moisture SMOS-L4 because of the distinct methodology used to obtain these products. Only SMOS descending passes or a mean between ascendant and descent passes are used to calculate mean daily values of SMOS-derived soil moisture. Soil moisture derived from the afternoon orbits was found to be more accurate than the morning passes (Piles et al. 2014). The fine temporal resolution of the model simulations (1 h) and the observations (10 min) allow comparisons at the time of the SMOS overpasses. Because of the 3-day revisit period of the SMOS swath, the IP will not be fully covered by the satellite on daily basis. However, despite identified difficulties (radio frequency interferences, missing data ...), the IP is well observed being 1.5 days the average observations frequency over the IP. Only those images with coverage higher than 50% are considered in our calculations. A conservative remapping to coarser resolutions is applied, when required, to make comparisons among each other or with respect to ground-based observations on equal terms. Remapping allows point to point comparisons between these data sets. In addition to the yearly and seasonal approach, an exemplary short time period, 19 to 20 October of 2012, is considered. This corresponds to one of the periods in which an extreme precipitation event occurred in the Ebro valley (at the end of November; Jansà et al. 2014. Therefore, high variability in the soil moisture distribution is expected.

The coefficient of variation (CV), defined as the ratio of the standard deviation to the mean, of the precipitation and soil moisture fields over the IP, the VAS (50x50 km2) and the OBS (10x10 km2) area are examined for the analysis of the spatial variability and its evolution in time. The soil moisture daily index ($SM_{index,i}$) is calculated to assess the evolution pattern allowing the study of daily variations

$SM_{index,i}= (SM_{i+1} -SM_i)/ SM_i$, where SM_{i+1} is the soil moisture of the day i+1 and SM_i is the soil moisture of the day before i.

For these calculations, SMOS afternoon (descendant; Piles et al. 2014) orbits are selected as well as observations at the time of the SMOS overpasses. For the IP and VAS, SMOS-L2 and SMOS–$L4^{3.0}$ have been remapped to the coarser grid spacing for an adequate comparison. Ground-based observations are aggregated using a mean over all stations for comparison with the corresponding SMOS-$L4^{3.0}$ data (the closest grid point is selected).

The reliability of SMOS-L3, SMOS-L2 and SMOS-$L4^{3.0}$ soil moisture products is evaluated by comparison with in situ soil moisture measurements in the OBS area. The spatial and temporal variability are considered as well as the probability distribution. Different approaches are applied: (a) the nearest grid point is selected for point-like comparisons between SMOS-L2 and SMOS-$L4^{3.0}$ against in situ soil moisture stations, to reduce sampling biases in this region of diverse soil characteristics (Table 1), (b) SMOS-$L4^{3.0}$ soil moisture grid cells are averaged over the 10x10 km^2 area and compared to the mean from the soil moisture network stations to address the issue related to spatial averaging due to the high spatial and temporal variability of the upper-most SSM. For the comparison between the SMOS-L2 and the in situ observations: when single ground-based stations are considered the closest SMOS pixel is selected, in case of considering the OBS (10x10 km^2) or VAS (50x50 km^2) areas the mean over all pixels which centre falls within the area is used. For the comparison with SMOS descending passes the corresponding values from in situ measurements are considered. Additionally, a separation between wet days (precipitation over 1 mm/d) and dry days is applied to consider possible implications of wet/dry soils for SMOS measurements.

Linear regression, the coefficient of determination (R^2), the mean bias (MB), and the root mean square deviation (RMSD) are used to predefine the accuracy. A debiased or centred RMSD (CRMSD) is applied to discriminate the systematic and random error components removing the overall bias before calculating the RMSD.

Soil moisture modeling is performed by the use of the SVAT, SURFEX (Externalized Surface) – module ISBA (Interactions between Soil-Biosphere-Atmosphere) from Météo-France. Configuration and specifications described in Juglea et al. (2010), which proved successful in adequately simulate the associated soil moisture heterogeneity over the wide VAS surface (50x50 km^2), are adapted in this study. Simulations start on 1 December 2011 at 00UTC and cover the whole investigation period until 31 December 2012 with an hourly-output time resolution. Point-scale SURFEX(ISBA) simulations over the soil moisture network stations in the VAS domain are validated with the in situ measurements to assess the usefulness of the model for further investigation, picturing the potential of the model in simulating upper level soil moisture variability on different soil characteristics (Table 1).

To try to simulate the spatial and temporal heterogeneity of the soil moisture fields over the VAS surface, the SURFEX(ISBA) scheme is used in combination with high quality forcing data from ECMWF (hereafter SURFEX-ECMWF) and the SAFRAN system (hereafter SURFEX-SAFRAN) for spatialization purposes. Soil moisture initialization in spatialized SURFEX(ISBA) simulations requires a single representative value for the whole simulation area. The benefit of initializing the simulations with SMOS-L4$^{3.0}$ data in comparison to climatological means is discussed. In-situ soil moisture observations over the VAS area are considered for verification. A comparison between SURFEX-SAFRAN point-scale and 10x10 km^2 mean simulations initialized with SMOS-L4$^{3.0}$ data is done against ground measurements to assess the accuracy of the simulated SSM maps.

4. Results

4.1 SMOS-derived soil moisture at different resolutions

4.1.1 Spatial variability on seasonal and sub-seasonal time scales

Figure 2a shows the north-south precipitation gradient for the SON period mean. The SSM satisfactorily reflects this gradient (Figure 2b), but, more markedly for the SMOS-L3 and SMOS-L2 than the higher resolution SMOS-L4$^{3.0}$ showing lower standard deviation, SMOS-L3(~0.15±0.01), SMOS-L2(~0.17±0.01), SMOS-L4(~0.22±0.007). The same performance is seen over the VAS domain (not shown). The SSM variability associated to the extreme precipitation events in this period is not well represented in the SMOS-L4$^{3.0}$ seasonal mean. Table 2 shows the number of days (percentage) in which there is more than 50 % of data over the IP for each SMOS product. These periods have been used as basis for the calculation of the spatial distributions in Figure 2b. SMOS-L3 (88 %) and SMOS-L2 (84 %) show a good coverage and similar number of days. However, a large difference is observed with respect to the SMOS-L4$^{2.0}$ product with only 28 days (32 %) of adequate coverage for the period of SON 2012. This is due to the problematic associated to the downscaling approach used to obtain the 1 km soil moisture maps, in which the lack of Land Surface Temperature (LST) information from MODIS visible/infrared (VIS/IR) satellite data in cloudy conditions (section 2.2) constrains derived-SSM information. The availability and usefulness of this product is therefore significantly reduced. The new product $L4^{3.0}$, used in this study, in which the previous limitation is resolved using ERA-Interim-derived LST information, shows a coverage percentage in the order of 92 %, even higher than the SMOS-L3 and -L2 products. However, Figure 2b demonstrates that the spatial representation of the seasonal mean does not improve with this product, as a consequence of the limited temporal availability of the SMOS-derived SSM product dictated by the revisit period of the satellite.

In Figure 3, only common available days from all different operational levels are selected for an inter-SMOS product comparison. When remapped to the same resolution (coarser grid spacing) comparable values are identified between SMOS-L3, -L2 and $–L4^{3.0}$ for the JJA and SON period, whereas relevant differences are pointed out from December to May. In this last period, we identify higher means for the SMOS-$L4^{3.0}$ product and SMOS-L3 with respect to SMOS-L2, which is in agreement with a systematic dry bias identified for SMOS-L2 also in previous studies (section 1).

At sub-seasonal scales, e.g. event scale on the 19-20 November 2012 (Figure 4), the SMOS-$L4^{\mathbf{3.0}}$ product shows SSM mean and variability in the same range of the SMOS-L2 and -L3 products, but with a finer-improved resolution representation of the spatial distribution. Comparisons with the mean ground-based SSM at the VAS (OBS area: *0.25 ±0.0002*) show better agreement with the mean SSM from the SMOS-$L4^{3.0}$-1 km disaggregated product (*0.23±0.002*) and poorer correlation with SMOS-L2 (*0.20±0.002*). The problematic of SMOS-$L4^{3.0}$ on seasonal time scales vanishes at sub-seasonal (event) scales where the potential added value of the 1 km product is manifest.

4.1.2 Temporal evolution of surface soil moisture data sets

The SMOS and in situ measured SSM time series are investigated and compared in this section in Figures 5 and 6 over the IP, the VAS (50x50 km2) and the OBS (10x10 km2) areas. Overall, the averaged SMOS-L2 and -L4$^{3.0}$ data over the IP are much more variable than the SMOS-L3, showing a more extreme daily index (SMOS-L2: -1 to 2; SMOS-L4$^{3.0}$: -0.7 to 1.45). Over the VAS, SMOS-L2 is clearly more variable than the higher resolution SMOS-L4$^{3.0}$. But, the last one shows a wider range of values as well as more extreme daily index values when compared to the averaged in situ soil moisture measurements. The CVs of the spatially averaged SMOS-L4$^{3.0}$ is lower than those of SMOS-L3, -L2 and in situ observations indicating that this data are less scattered. Despite detected differences within in situ observations, SMOS responds well to soil moisture variations over time.

Although absolute values are not totally captured, all three SMOS products adequately reproduce the temporal dynamics at a regional scale. The systematic dry bias present on SMOS-L2 data (Piles et al. 2014) is evident particularly on the first half of the year. A mean bias in the order of -0.09 to -0.07 m^3/m^3 is identified for the DJF-MAM period; this difference is reduced to -0.02 m^3/m^3 for the JJA-SON period (Table 3). During the DJF-MAM period the vineyards are bare, only the vine stocks are present. The water content of the vine stocks negatively impacts the SMOS measurements (Schwank et al. 2012).

Good agreement is found between the SMOS-L4$^{3.0}$ product and the mean of the in situ observations (the network's variability (shaded grey) contains the SMOS-L4$^{3.0}$ data). Scores confirm this result particularly for the periods DJF and SON (slope~1, R^2~0.7). Poorer correlation is found for the MAM (slope~0.6, R^2~0.4). In this period, soil moisture maxima immediately after the precipitation events are not always well captured by the SMOS-L4$^{3.0}$ data, showing additionally a too rapid drying after this. This observation agrees with the SMOS' inability of correctly measuring in situations when liquid water is present at the soil. The measured signal is perturbed during the vegetation growing season, which could explain the worse statistics. On the other hand, during JJA, low slope~0.1 and R^2~0.01 could be in relation to SSM values close to or lower than 0.1 m^3/m^3 and very low spatial variability, which was found to be necessary for an adequate performance of the algorithm used for the derivation of the SMOS-L4 1 km product in Molero et al. (2016).

4.2 Spatial comparison at high-resolution: SMOS-L4$^{3.0}$ versus ground measurements

High-resolution spatio-temporal correlations are assessed by spatial comparison with in situ observations. Characteristics of each of the in-situ stations are presented in Table 1. A seasonal analysis is performed focusing on the selected year of measurements covering a complete hydrological cycle (from 1 December 2011 to 31 December 2012). Comparisons between SMOS-L2 and ground measurements are additionally included. Statistics for individual comparisons at all stations are summarized in Table 3. Comparisons between SMOS-L3 and ground measurements were similarly performed evidencing the expected bad correlations (R^2 ~ 0,002, not shown)In Figure 7, the scatter plots display (a) possible differences between dry and wet days (> 1 mm/d), and (b, c) the agreement between remotely sensed and in situ soil moisture measurements from the OBS network using the seasonal classification. To consider any uncertainties arising from spatial averaging, ground measurements are compared to point like and 10x10 km^2 SSM means. The 10x10 km^2 area used covers the OBS area, i.e., the network of in situ measurements within the VAS. For comparison, all grid points from SMOS-L4$^{3.0}$ and SMOS-L2 included within the area are considered.

In Figure 7a, the separation between days with and without precipitation (< 1 mm/d) points out similar correlations during dry than wet days (RMSD~0.015, R^2~0.7) for SMOS-L4$^{3.0}$, whereas a slightly better agreement is found for the dry days (not shown) for SMOS-L2. A systematic mean dry bias of about 0.05 (dry days) to 0.08 (wet days) m^3/m^3 is assessed for SMOS-L2, while a lower bias with changing sign is identified for the L4$^{3.0}$ product (~ 0.005

(wet days); ~ -0.02 (dry days)). Comparisons using the corresponding mean over the 10x10 km^2 OBS area, in Figure 7b and Table 3, show good agreement with respect to the SMOS-$L4^{3.0}$ and poorer scores for SMOS-L2 (only one grid point of SMOS-L2 is located within the OBS area). Worse consistency is found in both cases for the MAM and JJA periods. CRMSD is in all cases in the required range of ≤ 0.04 m^3/m^3. Point-like comparisons with the individual in situ stations, in Figure 7c and Table 3, show that spatial patterns are captured at 1km with RMSD~0.007 to 0.1 m^3/m^3 but, in most cases, accuracy for SMOS-$L4^{3.0}$-1 km disaggregated product is within the required range of less than 0.04 m^3/m^3 (not shown). Higher RMSD is found for SMOS-L2, ~ 0.008 to 0.13 m^3/m^3, accounting for the previously identified dry bias (~ (-0.14) – (-0.02)) reduced in SMOS-$L4^{3.0}$ (~ (-0.08) – (-0.01)). The CRMSD is in all cases ≤ 0.04 m^3/m^3. For all stations, better correlations are found in DJF and SON and poorer scores in JJA and MAM, in agreement with the areal-mean comparisons (section 4.1.3). Best scores are obtained for Nicolas, VAS and La Cubera stations, probably in relation to their common soil type distribution, over vineyards, and homogeneous conditions, over a plain (Figure 8a, Table 3). The SON time period reveals the best agreement, at this time the vineyards are completely grown (however, senescent thus containing less water) and SSM exhibits substantial spatial variability driven by precipitation and irrigation thus improving spatio-temporal correlations. Worse statistics are found for Melbex-I, Melbex-II and Ezpeleta, probably in relation to the location of the soil moisture probes in rockier and orographically more complex areas, also in proximity to forestall and man-made construction areas.

The soil moisture probability distribution function (PDF; Figure 8b) of all in situ measurements versus SMOS-$L4^{3.0}$ data reveals that the later overestimates SSM below 0.1 m^3/m^3, values mainly observed during the JJA period. But, an underestimation occurs in the range between 0.1 and 0.3 m^3/m^3, which is consistent with the identified underestimation of maximum soil moisture reached after a precipitation event and the rapid drying of the soil in comparison to the much slower response seen in the observations during the MAM period (Figure 6c).

4.3 SURFEX model simulations and realistic initialization with 1-km soil moisture data

4.3.1 SURFEX model simulations of selected stations and realistic initialization

As a first step, the performance of the SURFEX(ISBA) SVAT model is evaluated. SURFEX(ISBA) point-like simulations are performed for all in situ soil moisture stations at the VAS area to assess the usefulness of the model for further investigation (Table 4).

SURFEX(ISBA) simulations show good agreement with soil moisture ground-based observations at all stations, adequately capturing the associated spatio-temporal variability (slope~1, R^2~ 0.7 to 0.9; MB~0.1 m^3/m^3; CRMSD~0.02 m^3/m^3). It can be concluded that the model performs well and is therefore suitable for further investigation. The seasonal analysis points out the best simulations in the SON period (R^2~0.9 for all stations), but CRMSD is ≤ 0.04 m^3/m^3 for all stations at all periods.

Using the mean of the ground-based measurement on the day of the model simulation initialization (realistic initialization; REAL-I) the temporal mean comparison for each station presented in Figure 9 and Table 4 reveals mean R^2~0.8 when the all hydrological year is considered.

4.3.2 Spatialization

As a first step, point-scale SURFEX-ECMWF and SURFEX-SAFRAN simulations covering the whole investigation period are performed for all in situ soil moisture stations to examine its ability to reproduce soil moisture dynamics. Ground measurements at each station are used for initialization. Scores clearly indicate better agreement with all in situ observations for the

SURFEX-SAFRAN simulations (slopes~ 1, R^2~ 0.9, RMSD< 0.1 m^3/m^3), rather than the SURFEX-ECMWF simulations (slopes> 1, R^2~ 0.6, and RMSD> 0.1 m^3/m^3).

In a second step, SURFEX-ECMWF and SURFEX-SAFRAN simulations are spatialized to obtain maps of soil moisture over the investigation area. In our CTRL simulations, the daily soil moisture from the mean of the in-situ measurements on the initialization day is used for model initialization. Mean SSM from in situ measurements for the whole investigation period is in the order of 0.14±0.005, whereas SURFEX-ECMWF derived SSM field is about 0.18±0.007 and SURFEX-SAFRAN derived SSM field is 0.15±0.002, thus, closer to ground-based observations. Performing a seasonal analysis, we demonstrate that this consistency is maintained for all seasons (not shown). The higher resolution of the SAFRAN-atmospheric forcing better reproduces the high spatial heterogeneity over the VAS area resulting in improved mapping of simulated SSM.

To exemplify the importance and implications of soil moisture initialization several experiments are performed. Initialization of the SURFEX-SAFRAN simulation using SMOS-$L4^{3.0}$ (EXP-SMOS) is examined against a sensitivity simulation using for the initial soil moisture scenario the climatological soil moisture from observations (daily mean over 10 years, which has been selected to be far from observations; EXP-CLIM). These experiments are initialized in dry periods, following Khodayar et al. (2014) recommendations, to maximize the impact, and run for about 3-4 months. In the first case, initialization is performed in a winter month (December) and the whole simulation period remains almost dry. In the second case, a summer month (July) is chosen for the initialization and it is followed by a wet autumn period with frequent heavy precipitation events in the area.

The temporal evolution of the RMSD (Figure 10a) demonstrates that the initial soil moisture scenario influences its evolution until the end of the simulation, in agreement with previous results in section 4.3.1. Larger deviations occur during dry periods, in both scenarios. Longer spin-up times, defined as the time that soil needs to re-establish quasi-equilibrium, characterize the dry scenario. It is after heavy precipitation events that deviations decrease. Soil quickly reacts to changes in the precipitation field in the semi-arid IP. When the upper level soil gets close to saturation soil memory is almost lost. Before the high precipitation events, SSM evolves following the direction of the initial perturbation, i.e., higher initial SSM yields higher SSM, however, a stochastic behaviour is identified afterwards.

As an example, differences in the spatial distribution of soil moisture for the winter/dry period simulation are discussed (Figure 10b). A relevant difference in the mean is identified when compared to the CTRL simulation (0.17±0.004): EXP-CLIM (0.014±0.003), EXP_SMOS (0.17±0.003). Clearly, better agreement is found in this last case.

Considering the EXP-SMOS initialization scenario simulation, a comparison between simulated point-like and the 10x10 km^2 mean against corresponding ground measurements was done for verification (Figure 10c). Correlations in the order of R^2~0.9 confirm that the combined use of SURFEX-SAFRAN and SMOS-$L4^{3.0}$ for initialization successfully reproduces soil moisture spatial and temporal variability becoming an optimal tool for mapping soil moisture heterogeneity over a study region for diverse purposes.

5. Discussion and conclusions

High-resolution soil moisture products are essential for our understanding of hydrological and climatic processes as well as improvement of model skills. Due to its high spatial and temporal variability, it is a complicated variable to assess. Mapping high-resolution soil moisture fields using intensively collected in-situ measurements is infeasible. Thus, state of the art high-resolution modelling and satellite-derived products have to fill this gap, although verification is needed. In this study, we examine the potential of the state of the art SMOS-

$L4^{3.0}$-1 km "all weather" disaggregated product for assessment of soil moisture variability, and improvement of the SVAT SURFEX(ISBA) simulations, in combination with the SAFRAN meteorological analysis system (SURFEX-SAFRAN), through realistic initialization. A dense network of ground-based soil moisture measurements over the Valencia Anchor Station (VAS; one of the SMOS test sites in Europe) is used for verification. The proposed analysis focuses on the semi-arid IP and covers the one year period of 2012 (from December 2011 to December 2012). The comparison of the SMOS-$L4^{3.0}$-1km product to different grid spacing soil moisture data products from SMOS, namely SMOS-L3 (~ 25 km) and SMOS-L2 (~15 km) shows that on seasonal time scales SMOS-$L4^{3.0}$ does not accurately capture the spatial variability of the soil moisture field, contrary to SMOS-L3 and SMOS-L2, despite the novelty of introducing ERA-Interim LST data in the MODIS LST/NDVI space (Piles et al. 2014; Sanchez-Ruiz et al. 2014). This is probably in relation to the so different spatial resolution of ERA-Interim and MODIS. This new downscaling approach greatly enhances the potential applicability of the data for those days/periods in which measurements are available, but cannot accurately fill in those periods without measurements dictated by the revisit period of the SMOS satellite, hence, compromising the soil moisture representation as a mean for longer periods than a day. On sub-seasonal time scales, when SMOS images are available, the SMOS-$L4^{3.0}$ high-resolution product shows its potential. It adequately captures the surface soil moisture variability in association with the precipitation field, also when extreme precipitation takes place.

Mean and single station comparisons with in-situ measurements reveal that characteristics of SMOS-$L4^{3.0}$ soil moisture fields are closer to in-situ observations than SMOS-L3 and -L2 products. Point-like and 10x10 km^2 comparisons show good agreement with respect to the SMOS-$L4^{3.0}$ and poorer scores for SMOS-L2 (e.g. DJF period: SMOS-L3/-L2: Slope:1.1/1.0, R^2:0.5/0.7, Bias:-0.09/(-0.03)). Generally, all three SMOS products adequately reproduce the soil moisture temporal dynamics meeting the desired accuracy of the mission (0.04 m3/m3); however, the spatial patterns did not always reach the expected precision in agreement with former studies in other regions (Gonzalez-Zamora et al. 2015). Comparisons with ground soil moisture measurements from the eight stations in the OBS network (10x10 km^2) over the VAS area shows that the spatial patterns are captured at 1 km with RMSD~ 0.007 to 0.1 m^3/m^3. The best correlations are in DJF and SON, and poorer scores in MAM and JJA, in agreement with the areal-mean comparisons. SMOS-$L4^{3.0}$ data shows better agreement at those stations over plain areas and with uniform conditions (vineyards), against those over more complex and less homogeneous terrains (rocky soils and areas close to forestall and man-made constructions). The SMOS-$L4^{3.0}$ soil moisture probability distribution function (PDF) in comparison to that of the in-situ measurements reveals a SMOS overestimation below 0.1 m^3/m^3 and an underestimation in the range between 0.1 to 0.3 m^3/m^3. A seasonal analysis points out better scores for the DJF and SON periods, whereas poorer correlation is found for the MAM and JJA periods. In the MAM period, an under-representation of the rainy events is found, as well as faster and stronger drying changes coinciding with the vegetation growth season. In JJA, the very low soil moisture values (< 0.1 m^3/m^3) with associated low spatial variability results in low R^2. No significant differences are found during dry and wet days (> 0.1 mm/d).

SURFEX(ISBA) SVAT simulations covering the whole investigation period over all in-situ measurement stations at the VAS area show good agreement with ground-based observations. Mean values are well reproduced for all stations and the temporal variability is well captured (R2~0.7 to 0.95; RMSD~0.02). The synergetic use of SURFEX(ISBA) simulations with SAFRAN atmospheric forcing information initialized with realistic SSM values from the SMOS-$L4^{3.0}$ data set was successful combination to obtain soil moisture maps over the VAS domain. Good agreement was reached when comparisons between point-like and 10x10 km^2

simulations with SURFEX-SAFRAN initialized with SMOS-L4$^{3.0}$ data and in-situ soil moisture measurements were made (R^2~0.9 and RMSD<0.04 m^3/m^3).

In this study, the comparison and suitability of different operational satellite products from the SMOS platform is investigated to provide realistic information on the water content of the soil. The comparison carried out helps drawing guidelines on best practices for the sensible use of these products. Currently, there is not a consensus about what is the "best" SMOS product. Different users utilize different products depending on their application rather than based on performance arguments. This study and the conclusions obtained on the comparison are important to provide information on the advantages and drawbacks of these datasets. The high temporal and spatial resolution soil moisture maps obtained in this study could be of use for hydrological and agronomical applications, to build climatologies of SSM, as initial condition for convective system modelling, for flood forescasting and for downstream local applications such as crop monitoring and crop development strategies as well as for irrigation data sets, among others. Additionally, an accurate representation of SSM will permit the calculation of SM profiles by application of e.g. exponential filters, which has been demonstrated to be a successful technique. Furthermore, the added value of the SMOS-L4$^{3.0}$-1 km disaggregated product for initialization purposes is demonstrated, which suggests its potential for assimilation purposes. These two last aspects are out of the scope of this paper, but they are investigated in detail in a follow-up study. Important aspects of the SMOS-L4$^{3.0}$ SSM product have still to be improved, namely its temporal availability (e.g. successful investigations on the increase of SMOS-L3 temporal resolution to 3h are available (Louvet et al. 2015)), its spatio-temporal correlation with in situ measurements over complex topographic areas, in areas/periods with low spatial variability and in rainy periods when an under-representation and rapid decay of SSM has been identified.This study also points out that in order to more accurately examine the reproducibility of the high spatial variability of this variable by the newly available satellite derived downscaled high-resolution soil moisture observations, large and dense networks of in situ soil moisture measurements covering different soil types and land uses as well as considering different soil depths are needed. In an effort to come a step forward in this direction, dedicated long-term networks with the previously described characteristics should be established permanently in different regions around the world.

Acknowledgements

The authors acknowledge AEMET for supplying the precipitation data and the HyMeX database teams (ESPRI/IPSL and SEDOO/Observatoire Midi-Pyrénées) for their help in accessing the data. The SMOS products were obtained from CATDS (Centre Aval de Traitement des Données SMOS) and SMOS-BEC (Barcelona Expert Center. We acknowledge the support of the SURFEX-web team members. The ECMWF data was obtained from http://www.ecmwf.int. Special thanks go to Pere Quintana for providing the SAFRAN atmospheric forcing data. A. Coll´s work was supported by both National Spanish Space Research Programme projects MIDAS-6 (MIDAS-6/UVEG. SMOS Ocean Salinity and Soil Moisture Products. Improvements and Applications Demonstration) and MIDAS-7 (MIDAS-7/UVEG. SMOS and Future Missions Advanced Products and Applications). The first author's research is supported by the Bundesministerium für Bildung und Forschung (BMBF; German Federal Ministry of Education and Research).

References

ARRAY Systems Computing Inc., CESBIO, IPSL-Service d'Aéronomie, INRA-EPHYSE, Reading University, Tor Vergata University. Algorithm Theoretical Basis Document (ATBD) for the SMOS Level 2 Soil Moisture Processor Development Continuation Project. ESA No.: SO-TN-ARR-L2PP-0037 Issue: 3.9 Array No.: ASC_SMPPD_037 Date: October 24, 2014

Bircher, S., Skou, N., Jensen, K. H., Walker, J. P., & Rasmussen, L. (2012). A soil moisture and temperature network for SMOS validation in Western Denmark. Hydrology and Earth System Sciences, 16(5), 1445-1463.

Bolle, H.-J., Eckardt, M., Koslowsky, D., Maselli, F., Meliá Miralles, J., Menenti, M., Olesen, F.-S., Petkov, L., Rasool, I., Van de Griend, A.A. (Editors). Contributing Authors: H. Billing, A. Gitelson, F. Göttsche, A. Jochum-Osann, E. Lopez-Baeza, F. Meneguzzo, J. Moreno, F. Nerry, P. Rossini, F. Veroustraete, R. Vogt, P.J. Van Oeleven. Mediterranean Landsurface Processes Assessed From Space. Chapter 6 From Research to Application. Regional Climate Studies Series. Springer-Verlag Berlin Heidelberg, ISBN: 978-3-540-40151-3 (Print) 978-3-540-45310-9 (Online) (2006)

Boone, A., Calvet, J.-C., & Noilhan, J. (1999). Inclusion of a Third Soil Layer in a Land Surface Scheme Using the Force–Restore Method. Journal of Applied Meteorology, 38, 1611–1630. https://doi.org/10.1175/1520-0450(1999)038<1611:IOATSL>2.0.CO;2

Bosch, D. D., J. M. Sheridan, and L. K. Marshall (2007), Precipitation, soil moisture, and climate database, Little River Experimental Watershed, Georgia, United States, Water Resour. Res., 43, W09472, doi:10.1029/2006WR005834

Brocca, L., Melone, F., Moramarco, T., Wagner, W., & Hasenauer, S. (2010). ASCAT soil wetness index validation through in situ and modeled soil moisture data in central Italy. Remote Sensing of Environment, 114(11), 2745-2755.

Calvet, J.-C., Noilhan, J., & Bessemoulin, P. (1998). Retrieving the Root-Zone Soil Moisture from Surface Soil Moisture or Temperature Estimates: A Feasibility Study Based on Field Measurements. Journal of Applied Meteorology, 37(1995), 371–386. https://doi.org/10.1175/1520-0450(1998)037<0371:RTRZSM>2.0.CO;2

Clapp, R. B., & Hornberger, G. M. (1978). Empirical equations for some soil hydraulic properties. Water resources research, 14(4), 601-604.

Cosby, B. J., Hornberger, G. M., Clapp, R. B., & Ginn, T. (1984). A statistical exploration of the relationships of soil moisture characteristics to the physical properties of soils. Water resources research, 20(6), 682-690.

Cosh, M. H., Jackson, T. J., Bindlish, R., & Prueger, J. H. (2004). Watershed scale temporal and spatial stability of soil moisture and its role in validating satellite estimates. Remote sensing of Environment, 92(4), 427-435.

Djamai, N., Magagi, R., Goïta, K., Merlin, O., Kerr, Y., Roy, A. (2016). A combination of DISPATCH downscaling algorithm with CLASS land surface scheme for soil moisture estimation at fine scale during cloudy days. Remote Sensing of Environment, 184, 1-14.

De Lannoy, G. J., & Reichle, R. H. (2016). Global assimilation of multiangle and multipolarization SMOS brightness temperature observations into the GEOS-5 catchment land surface model for soil moisture estimation. Journal of Hydrometeorology, 17(2), 669-691.

Delwart, S., Bouzinac, C., Wursteisen, P., Berger, M., Drinkwater, M., Martín-Neira, M., & Kerr, Y. H. (2008). SMOS validation and the COSMOS campaigns. IEEE Transactions on Geoscience and Remote Sensing, 46(3), 695-704.

Dente, L., Su, Z., & Wen, J. (2012). Validation of SMOS soil moisture products over the Maqu and Twente regions. Sensors, 12(8), 9965-9986.

Drobinski P., V. Ducrocq, P. Alpert, E. Anagnostou, K. Béranger, M. Borga, I. Braud, A. Chanzy, S. Davolio, G. Delrieu, C. Estournel, N. Filali Boubrahmi, J. Font, V. Grubišić, S.

Gualdi, V. Homar, B. Ivančan-Picek, C. Kottmeier, V. Kotroni, K. Lagouvardos, P. Lionello, M. C. Llasat, W. Ludwig, C. Lutoff, A. Mariotti, E. Richard, R. Romero, R. Rotunno, O. Roussot, I. Ruin, S. Somot, I. Taupier-Letage, J. Tintore, R. Uijlenhoet, and H. Wernli, 2014. HyMeX: A 10-year multidisciplinary program on the Mediterranean water cycle. Bull. Amer. Meteor. Soc., 95, 1063–1082. doi: http://dx.doi.org/10.1175/BAMS-D-12-00242.1

Ducrocq Véronique, Isabelle Braud, Silvio Davolio, Rossella Ferretti, Cyrille Flamant, Agustin Jansa, Norbert Kalthoff, Evelyne Richard, Isabelle Taupier-Letage, Pierre-Alain Ayral, Sophie Belamari, Alexis Berne, Marco Borga, Brice Boudevillain, Olivier Bock, Jean-Luc Boichard, Marie-Noëlle Bouin, Olivier Bousquet, Christophe Bouvier, Jacopo Chiggiato, Domenico Cimini, Ulrich Corsmeier, Laurent Coppola, Philippe Cocquerez, Eric Defer, Julien Delanoë, Paolo Di Girolamo, Alexis Doerenbecher, Philippe Drobinski, Yann Dufournet, Nadia Fourrié, Jonathan J. Gourley, Laurent Labatut, Dominique Lambert, Jérôme Le Coz, Frank S. Marzano, Gilles Molinié, Andrea Montani, Guillaume Nord, Mathieu Nuret, Karim Ramage, William Rison, Odile Roussot, Frédérique Said, Alfons Schwarzenboeck, Pierre Testor, Joël Van Baelen, Béatrice Vincendon, Montserrat Aran, and Jorge Tamayo, 2014. HyMeX-SOP1: The field campaign dedicated to heavy precipitation and flash flooding in the Northwestern Mediterranean. Bull. Amer. Meteor. Soc., 95, 1083–1100. doi: http://dx.doi.org/10.1175/BAMS-D-12-00244.1

Duffourg, F., & Ducrocq, V. (2011). Origin of the moisture feeding the Heavy Precipitating Systems over Southeastern France. Natural Hazards and Earth System Sciences, 11(4), 1163.

Duffourg, F., & Ducrocq, V. (2013). Assessment of the water supply to Mediterranean heavy precipitation: a method based on finely designed water budgets. Atmospheric Science Letters, 14(3), 133-138.

Durand, Y., E. Brun, L. Mérindol, G. Guyomarc'h, B. Lesaffre, E. Martin, A meteorological estimation of relevant parameters for snow models, Ann. Glaciol. 18 (1993) 65–71.

Durand, Y., G. Giraud, M. Laternser, P. Etchevers, L. Mérindol, B. Lesaffre, Reanalysis of 47 Years of Climate in the French Alps (1958–2005): Climatology and Trends for Snow Cover, J. Appl. Meteorol. Climatol. 48 (2009) 2487–2512.

Entekhabi, D., Rodriguez-Iturbe, I., & Castelli, F. (1996). Mutual interaction of soil moisture state and atmospheric processes. Journal of Hydrology, 184(1-2), 3-17.

Entekhabi, D.; Njoku, E.G.; Neill, P.E.; Kellogg, K.H.; Crow, W.T.; Edelstein,W.N.; Entin, J.K.; Goodman, S.D.; Jackson, T.J.; Johnson, J. The soil moisture active passive (SMAP) mission (2010). Proc. IEEE, 98, 704–716.

FAO; World reference base for soil resources 2014 international soil classification system for naming soils and creating legends for soil maps. Rome: FAO, 2014.

Gherboudj, I., Magagi, R., Goïta, K., Berg, A. A., Toth, B., & Walker, A. (2012). Validation of SMOS data over agricultural and boreal forest areas in Canada. IEEE Transactions on Geoscience and Remote Sensing, 50(5), 1623-1635.

GTOPO30 Documentation, U.S. Geological Survey, 1996, Global 30 Arc-Second Elevation

A. Gonzalez-Zamora, N. Sánchez, J. Martinez-Fernandez, A. Gumuzzio, M. Piles, E. Olmedo. Long-Term SMOS Soil Moisture Products: A Comprehensive Evaluation across Scales and Methods in the Duero Basin Physics and Chemistry of the Earth, Parts A/B/C, 83–84 (2015), pp. 123–136 http://dx.doi.org/10.1016/j.pce.2015.05.009

Hirschi, M., Seneviratne, S. I., Alexandrov, V., Boberg, F., Boroneant, C., Christensen, O. B., and Stepanek, P. (2011). Observational evidence for soil-moisture impact on hot extremes in southeastern Europe. Nature Geoscience, 4(1), 17.

Jansa, J., Erb, A., Oberholzer, H. R., Šmilauer, P., & Egli, S. (2014). Soil and geography are more important determinants of indigenous arbuscular mycorrhizal communities than management practices in Swiss agricultural soils. Molecular ecology, 23(8), 2118-2135.

Jones, M. O., L. A. Jones, J. S. Kimball, and K. C. McDonald (2011), Satellite passive microwave remote sensing for monitoring global land surface phenology, Remote Sens. Environ., 115(4), 1102–1114, doi:10.1016/j.rse.2010.12.015.

Juglea, S., Kerr, Y., Mialon, A., Lopez-Baeza, E., Braithwaite, D., & Hsu, K. (2010). Soil moisture modelling of a SMOS pixel: Interest of using the PERSIANN database over the Valencia Anchor Station. Hydrology and Earth System Sciences, 14(8), 1509–1525. https://doi.org/10.5194/hess-14-1509-2010

Juglea, S., Kerr, Y., Mialon, A., Wigneron, J. P., Lopez-Baeza, E., Cano, A., … Delwart, S. (2010). Modelling soil moisture at SMOS scale by use of a SVAT model over the Valencia Anchor Station. Hydrology and Earth System Sciences, 14(5), 831–846. https://doi.org/10.5194/hess-14-831-2010

Kerr, Y. H. (2007). Soil moisture from space: Where are we?. Hydrogeology journal, 15(1), 117-120.

Kerr, Y. H., Waldteufel, P., Wigneron, J. P., Delwart, S., Cabot, F., Boutin, J., ... & Juglea, S. E. (2010). The SMOS mission: New tool for monitoring key elements ofthe global water cycle. Proceedings of the IEEE, 98(5), 666-687.

Kerr, Y. H., Waldteufel, P., Wigneron, J. P., Martinuzzi, J. A. M. J., Font, J., & Berger, M. (2001). Soil moisture retrieval from space: The Soil Moisture and Ocean Salinity (SMOS) mission. IEEE transactions on Geoscience and remote sensing, 39(8), 1729-1735.

Khodayar, S., Raff, F., Kalthoff, N. 2015. Dignostic Study of a High Precipitation Event in the Western Mediterranean Region: Adequacy of Current operational Networks Quart. J. Roy. Meteor. Soc. DOI: 10.1002/qj.2600

Khodayar, S., Sehlinger, A., Feldmann, H., & Kottmeier, C. (2015). Sensitivity of soil moisture initialization for decadal predictions under different regional climatic conditions in Europe. International Journal of Climatology, 35(8), 1899-1915.

Koster, R. D., Dirmeyer, P. A., Guo, Z., Bonan, G., Chan, E., Cox, P., ... & Liu, P. (2004). Regions of strong coupling between soil moisture and precipitation. Science, 305(5687), 1138-1140.

Le Moigne, P., Boone, A., Calvet, J. C., Decharme, B., Faroux, S., Gibelin, A. L., ... & Mironov, D. (2009). SURFEX scientific documentation. Note de centre (CNRM/GMME), Météo-France, Toulouse, France.

Liu, Y.Y.; Parinussa, R.M.; Dorigo, W.A.; De Jeu, R.A.M.; Wagner, W.; van Dijk, A.I.J.M.; McCabe, M.F.; Evans, J.P. Developing an improved soil moisture dataset by blending passive and active microwave satellite-based retrievals (2011). Hydrol. Earth Syst. Sci., 15, 425–436.

Louvet, S., Thierry Pellarin, Ahmad al Bitar, Bernard Cappelaere, Sylvie Galle, Manuela Grippa, Claire Gruhier, Yann Kerr, Thierry Lebel, Arnaud Mialon, Eric Mougin, Guillaume

Quantin, Philippe Richaume, Patricia de Rosnay (2015). SMOS soil moisture product evaluation over West-Africa from local to regional scale. Remote Sensing of Environment, Volume 156, Pages 383-394, ISSN 0034-4257, DOI: 10.1016/j.rse.2014.10.005.

Malbéteau, Y., Merlin, O., Balsamo, G., Er-Raki, S., Khabba, S.,Walker, J. P., Jarlan, L. (2018). Toward a Surface Soil Moisture Product at High Spatiotemporal Resolution: Temporally Interpolated, Spatially Disaggregated SMOS Data. Journal of Hydrometeorology, 19(1), 183-200.

Masson, V., Champeaux, J. L., Chauvin, F., Meriguet, C., & Lacaze, R. (2003). A global database of land surface parameters at 1-km resolution in meteorological and climate models. Journal of Climate, 16(9), 1261–1282. https://doi.org/10.1175/1520-0442-16.9.1261

Merlin, O., Rüdiger, C., Al Bitar, A., Richaume, P., Walker, J. P., & Kerr, Y. H. (2012). Disaggregation of SMOS soil moisture in Southeastern Australia. IEEE Transactions on Geoscience and Remote Sensing, 50(5), 1556–1571. http://dx.doi.org/10.1109/TGRS. 2011.2175000.

Naeimi, V.; Scipal, K.; Bartalis, Z.; Hasenauer, S.; Wagner, W. An improved soil moisture retrieval algorithm for ers and metop scatterometer observations (2009). IEEE Trans. Geosci. Remote Sens. 47, 1999–2013.

Noilhan, J., & Planton, S. (1989). A Simple Parameterization of Land Surface Processes for Meteorological Models. Monthly Weather Review. https://doi.org/10.1175/1520-0493(1989)117<0536:ASPOLS>2.0.CO;2

Owe, M.; de Jeu, R.; Holmes, T. Multisensor historical climatology of satellite-derived global land surface moisture (2008). J. Geophys. Res. Earth Surf., 113, F01002.

Piles, M., Camps, A., Vall-Llossera, M., Corbella, I., Panciera, R., Rudiger, C., … Walker, J. (2011). Downscaling SMOS-derived soil moisture using MODIS visible/infrared data. IEEE Transactions on Geoscience and Remote Sensing, 49(9), 3156–3166. https://doi.org/10.1109/TGRS.2011.2120615

Piles, M., Sánchez, N., Vall-Llossera, M., Camps, A., Martínez-Fernandez, J., Martinez, J., & Gonzalez-Gambau, V. (2014). A downscaling approach for SMOS land observations: Evaluation of high-resolution soil moisture maps over the Iberian peninsula. IEEE Journal of Selected Topics in Applied Earth Observations and Remote Sensing, 7(9), 3845–3857. https://doi.org/10.1109/JSTARS.2014.2325398

Piles, M., Vall-Llossera, M., Camps, A., Sanchez, N., Martinez-Fernandez, J., Martinez, J., … Riera, R. (2013). On the synergy of SMOS and Terra/Aqua MODIS: High resolution soil moisture maps in near real-time. International Geoscience and Remote Sensing Symposium (IGARSS), 3423–3426. https://doi.org/10.1109/IGARSS.2013.6723564

Piles, M., Pou, X., Camps, A., Vall-llosera, M. (2015): Quality report: Validation of SMOS-BEC L4 high resolution soil moisture products, version 3.0 or "all-weather". Technical report. Available at: http://bec.icm.csic.es/doc/BEC-SMOS-L4SMv3-QR.pdf

Quintana-Segui, P., Le Moigne, P., Durand, Y., Martin, E., Habets, F., Baillon, M., ... & Morel, S. (2008). Analysis of near-surface atmospheric variables: Validation of the SAFRAN analysis over France. Journal of applied meteorology and climatology, 47(1), 92-107.

Quintana-Seguí, P., Peral, C., Turco, M., Llasat, M. C., & Martin, E. (2016). Meteorological Analysis Systems in North-East Spain: Validation of SAFRAN and SPAN. Journal of Environmental Informatics, 27(2).

Raveh-Rubin, S., and Wernli, H. (2015). Large-scale wind and precipitation extremes in the Mediterranean: a climatological analysis for 1979–2012. Quarterly Journal of the Royal Meteorological Society, 141(691), 2404-2417.

Robock, A., Vinnikov, K. Y., Srinivasan, G., Entin, J. K., Hollinger, S. E., Speranskaya, N. A., ... & Namkhai, A. (2000). The global soil moisture data bank. Bulletin of the American Meteorological Society, 81(6), 1281-1299.

Rosenbaum, U., H. R. Bogena, M. Herbst, J. A. Huisman, T. J. Peterson, A. Weuthen, A. W. Western, and H. Vereecken (2012), Seasonal and event dynamics of spatial soil moisture patterns at the small catchment scale, WaterResour.Res., 48, W10544, doi:10.1029/2011WR011518.

Sanchez N., J. Martinez-Fernandez, A. Scaini and C. Perez-Gutierrez, "Validation of the SMOS L2 Soil Moisture Data in the REMEDHUS Network (Spain)," in IEEE Transactions on Geoscience and Remote Sensing, vol. 50, no. 5, pp. 1602-1611, May 2012. doi: 10.1109/TGRS.2012.2186971

Sánchez-Ruiz, S., Piles, M., Sánchez, N., Martínez-Fernández, J., Vall-llossera, M., & Camps, A. (2014). Combining SMOS with visible and near/shortwave/thermal infrared satellite data for high resolution soil moisture estimates. Journal of Hydrology, 516, 273–283. https://doi.org/10.1016/j.jhydrol.2013.12.047

Schubert, M., & Boche, H. (2004). Solution of the multiuser downlink beamforming problem with individual SINR constraints. IEEE Transactions on Vehicular Technology, 53(1), 18-28.

Schwank, M., Wigneron, J. P., Lopez-Baeza, E., Volksch, I., Matzler, C., & Kerr, Y. H. (2012). L-band radiative properties of vine vegetation at the MELBEX III SMOS cal/val site. IEEE Transactions on Geoscience and Remote Sensing, 50(5), 1587-1601.

Seneviratne, S. I., Corti, T., Davin, E. L., Hirschi, M., Jaeger, E. B., Lehner, I., ... & Teuling, A. J. (2010). Investigating soil moisture–climate interactions in a changing climate: A review. Earth-Science Reviews, 99(3), 125-161.

SMOS-BEC Team (2016): SMOS-BEC Ocean and Land Products Description. Technical report. Available at: http://bec.icm.csic.es/doc/BEC-SMOS-0001-PD.pdf

Taylor, C. M., & Lebel, T. (1998). Observational evidence of persistent convective-scale rainfall patterns. Monthly Weather Review, 126(6), 1597-1607.

Vautard, R., Yiou, P., D'andrea, F., De Noblet, N., Viovy, N., Cassou, C., ... & Fan, Y. (2007). Summertime European heat and drought waves induced by wintertime Mediterranean rainfall deficit. Geophysical Research Letters, 34(7).

Vidal, J.-P., E. Martin, L. Franchistéguy, M. Baillon, J.-M. Soubeyroux, A 50-year high-resolution atmospheric reanalysis over France with the Safran system, Int. J. Climatol. 30 (2010) 1627–1644.

Wagner, W.; Dorigo, W.; de Jeu, R.; Fernandez, D.; Benveniste, J.; Haas, E.; Ertl, M. Fusion of active and passive microwave observations to create an essential climate variable data record on soil moisture (2012). ISPRS Ann. Photogramm. Remote Sens. Spat. Inf. Sci. 1–7, 315–321.

Walker, J., & Rowntree, P. R. (1977). The effect of soil moisture on circulation and rainfall in a tropical model. Quarterly Journal of the Royal Meteorological Society, 103(435), 29-46.

Western, A. W., Grayson, R. B., & Blöschl, G. (2002). Scaling of soil moisture: A hydrologic perspective. Annual Review of Earth and Planetary Sciences, 30(1), 149-180.

Wigneron, J. P., Calvet, J. C., Pellarin, T., Van de Griend, A. A., Berger, M., & Ferrazzoli, P. (2003). Retrieving near-surface soil moisture from microwave radiometric observations: current status and future plans. Remote Sensing of Environment, 85(4), 489-506.

Wigneron, J.-P., M. Schwank, E. Lopez Baeza, Y. Kerr, N. Novello, C. Millan, C. Moisy, P. Richaume, A. Mialon, A. Al Bitar, F. Cabot, H. Lawrence, D. Guyon, J-C Calvet, J. P. Grant, P. de Rosnay, A. Mahmoodi, S. Delwart, S. Mecklenburg (2012). First Evaluation of the Simultaneous SMOS and ELBARA-II Observations in the Mediterranean Region. Remote Sensing of Environment, 124, 26–37

Zampieri, M., F. D’Andrea, R. Vautard, P. Ciais, N. de Noblet-Ducoudré, and P. Yiou, 2009: Hot European Summers and the Role of Soil Moisture in the Propagation of Mediterranean Drought. J. Climate, 22, 4747–4758, https://doi.org/10.1175/2009JCLI2568.1

Tables

Table 1: Characteristics of soil moisture stations within the VAS domain.

NAME	STATION	DOMINANT VEGETATION USED FOR SIMULATIONS	TYPE OF VEGETATION	SAND	SILT	CLAY	ALTITUDE (m)	ANNUAL MEAN TEMPERATURE (ºC)	ANNUAL MEAN PRECIPITATION (mm)
Melbex_I		Schrub	Schrub	0,47	0,38	0,15	849	(12-14)	451
Nicolas		Vineyard	Schrub/ Vineyard	0,47	0,35	0,18	859		
La Cubera		Vineyard	Vineyard	0,45	0,35	0,20	762		
Ezpeleta		Olive tree	Olive tree	0,44	0,39	0,17	781		
VAS		Vineyard	Vineyard	0,46	0,37	0,17	804		
Melbex_II		Vineyard	Vine stump/ Vine row	0,45	0,29	0,26	797		

Table 2: Number of days (percentage) in which the SMOS (ascendant and descendent swaths) coverage is higher than 50 %.

LEVEL SMOS	SEPTEMBER		OCTOBER		NOVEMBER		SON	
	days	%	days	%	days	%	days	%
$L4^{2.0}$ (~1km)	10	34	9	31	9	31	28	32
$L4^{3.0}$ (~1km)	23	74	29	90	30	100	82	92
L2 (~15km)	20	67	28	90	28	93	76	83
L3 (~25km)	22	73	29	93	29	96	80	88

Table 3: Statistics of the comparisons between SMOS-L2 and SMOS-L4$^{3.0}$ soil moisture versus ground-based measurements in the VAS network (the area covering the ground-based network has been called OBS, Figure 1). SMOS descendent orbits are selected for the comparison. Characteristics of the individual stations are given in Table 1. The acronyms for the names of the stations are as follows: (M-I: Melbex_I, M_II: Melbex_II, VAS: VAS, NIC: Nicolas, EZ: Ezpeleta, LC: La Cubera). The period December 2011 to December 2012 is evaluated. The seasonal analysis follows the hydrological cycle. OBS stands for the average of (i) SMOS-L2 and/or SMOS-L4$^{3.0}$ soil moisture values within the 10x10 km^2 where the ground-based network is placed, and (ii) in the case of the in situ observations it refers to the mean of all stations. In Table (a) a seasonal comparison between the mean of all in situ stations and the corresponding mean of SMOS-L2 and/or SMOS-L4$^{3.0}$ soil moisture values within the 10x10 km^2 area. In (b) SMOS-L2 and SMOS-L4$^{3.0}$ soil moisture observations are compared to point-like ground measurements using the closest grid point. The column on the right shows the mean of all stations

(a)

OBS vs SMOS-L2	**Slope**	**R2**	**Bias**	**CRMS**	**OBS vs SMOS-L4$^{3.0}$**	**Slope**	**R2**	**Bias**	**CRMS**
DJF	1.1	0.5	-0.09	0.03	**DJF**	1.0	0.7	-0.03	0.04
MAM	0.6	0.2	-0.07	0.03	**MAM**	0.6	0.4	-0.03	0.03
JJA	0.3	0.01	-0.02	0.03	**JJA**	0.1	0.01	-0.003	0.03
SON	1.1	0.8	-0.02	0.04	**SON**	0.8	0.7	-0.003	0.04

(b)

SMOSL2 vs SMOSL4$^{3.0}$	**M-I**	**M-II**	**VAS**	**NIC**	**EZ**	**LC**	**OBS (mean all stations)**
				DJF			
Slope	0.17/-0.04	1.0/1.7	1.6/2.3	1.1/1.7	0.8/0.9	0.9/1.7	1.1/0.6
R2	0.02/0.01	0.6/0.5	0.8/0.5	0.9/0.7	0.5/0.2	0.7/0.7	0.5/0.7
MB	-0.03/-0.08	-0.08/-0.14	0.01/-0.04	0.006/-0.05	0.03/-0.02	0.004/-0.05	-0.09/-0.03
CRMSD	0.04/0.03	0.03/0.02	0.04/0.03	0.03/0.03	0.04/0.03	0.04/0.03	0.03/0.04
				MAM			
Slope	0.4/0.36	0.6/0.4	0.8/0.6	0.6/0.8	0.5/0.3	0.9/0.7	0.6/0.6
R2	0.2/0.08	0.3/0.04	0.5/0.15	0.9/0.5	0.3/0.14	0.4/0.2	0.2/0.4
MB	-0.04/-0.08	-0.08/-0.11	0.005/-0.03	0.003/-0.03	0.02/-0.02	-0.02/-0.05	-0.07/-0.03
CRMSD	0.03/0.03	0.03/0.03	0.03/0.03	0.03/0.03	0.04/0.03	0.03/0.03	0.03/0.03
				JJA			
Slope	0.26/0.38	0.3/0.4	0.02/0.15	0.1/0.3	0.08/-0.04	0.05/0.06	0.3/0.1
R2	0.02/0.01	0.04/0.005	0.001/0.002	0.8/0.17	0.003/0.012	0.01/0.003	0.01/0.01
MB	-0.01/-0.03	-0.04/-0.05	0.03/0.012	0.01/0.002	0.05/0.04	0.03/0.02	-0.02/-0.003
CRMSD	0.03/0.03	0.03/0.03	0.03/0.03	0.03/0.03	0.03/0.03	0.03/0.03	0.03/0.03
				SON			
Slope	0.69/1.06	0.9/1.3	1.2/1.7	0.8/1.2	0.7/1.1	0.8/1.3	1.1/0.8
R2	0.5/0.6	0.6/0.6	0.7/0.8	0.9/0.7	0.8/0.7	0.8/0.7	0.8/0.07
MB	-0.02/-0.04	-0.03/-0.05	0.04/-0.03	0.03/0.006	0.03/0.01	0.04/0.02	-0.02/-0.003
CRMSD	0.04/0.04	0.04/0.04	0.04/0.04	0.04/0.04	0.04/0.04	0.04/0.04	0.04/0.04

Table 4: Statistics of daily areal averages of ground-based SSM measurements in the OBS area versus point-like SURFEX(ISBA) simulations at the same sites. The acronyms for the names of the stations are as described in Table 3.

	M-I	M-II	VAS	NIC	EZ	LC	OBS
All period							
Slope	0.9	1.3	0.9	0.7	1.0	0.9	1.0
R2	0.8	0.8	0.8	0.8	0.8	0.7	0.9
MB	0.004	-0.012	0.011	0.006	0.02	0.006	0.005
CRMSD	0.02	0.02	0.02	0.02	0.01	0.02	0.02
DJF							
Slope	0.2	1.3	0.8	1.2	1.2	1.1	1.1
R2	0.03	0.4	0.4	0.7	0.7	0.5	0.6
MB	0.01	-0.03	0.02	0.03	0.02	0.03	0.01
CRMSD	0.04	0.05	0.03	0.04	0.03	0.03	0.04
MAM							
Slope	0.8	1.0	1.0	0.7	0.8	0.7	0.9
R2	0.5	0.4	0.6	0.4	0.6	0.5	0.6
MB	0.002	-0.02	0	0.01	0.01	-0.02	-0.004
CRMSD	0.04	0.02	0.03	0.04	0.03	0.04	0.04
JJA							
Slope	0.4	0.8	1.6	3	1.6	2	1.5
R2	0.7	0.8	0.7	0.5	0.7	0.6	0.8
MB	0.004	0.01	0.01	-0.02	0.02	0.005	0.005
CRMSD	0.04	0.02	0.03	0.04	0.03	0.04	0.04
SON							
Slope	0.9	1.1	0.9	0.8	1.0	1.1	1.0
R2	0.8	0.8	0.8	0.9	0.9	0.8	0.9
MB	0.002	0	0.01	0	0.02	0.01	0.006
CRMSD	0.04	0.006	0.03	0.04	0.04	0.03	0.04

Figures

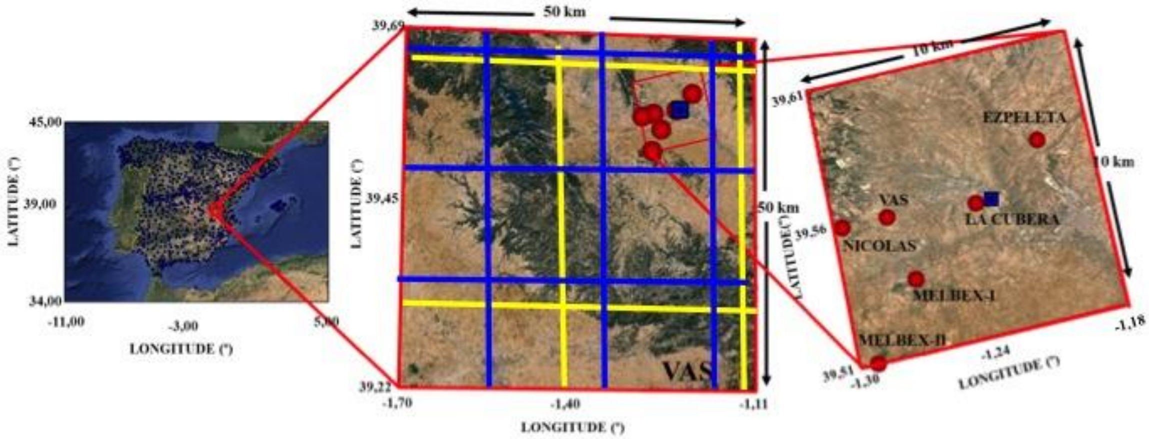

Figure 1: Area of investigation and orography. Location of rain gauges from AEMET (Meteorological Service of Spain) is shown over the Iberian Peninsula (blue square dots). The positions of the soil moisture network stations within the 10x10 km^2 (OBS area) in the Valencia Anchor Station (VAS; 50x50 km^2) area are indicated by red circles.

(a)

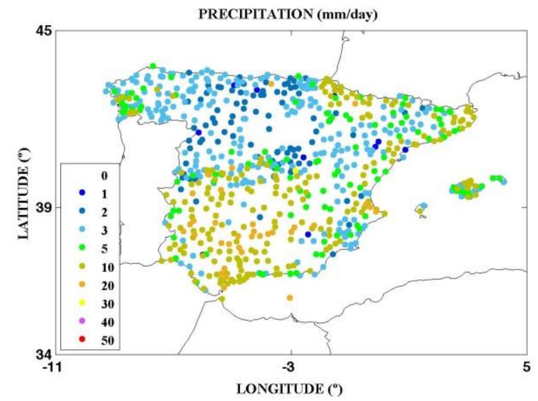

(b)

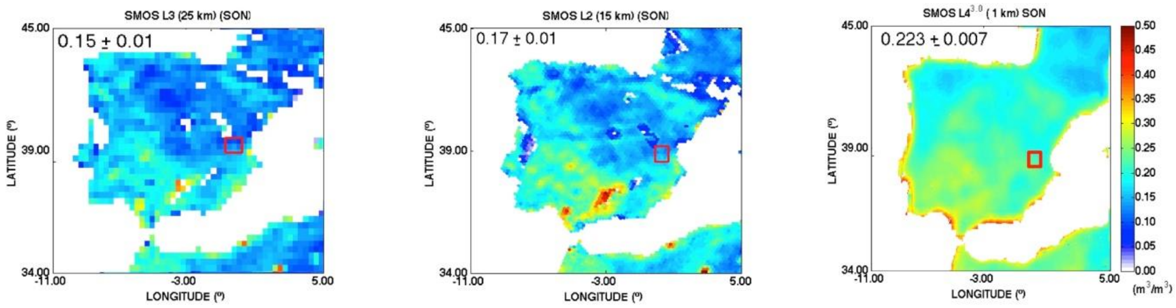

Figure 2: (a) Spatial distribution of precipitation over the Iberian Peninsula from the network of rain gauges of AEMET. The period of September to November (SON) 2012 is shown. (b) Spatial distribution of SMOS-derived soil moisture over the Iberian Peninsula (merged product: ascending and descending orbits, days with areal coverage higher than 50 % are considered).

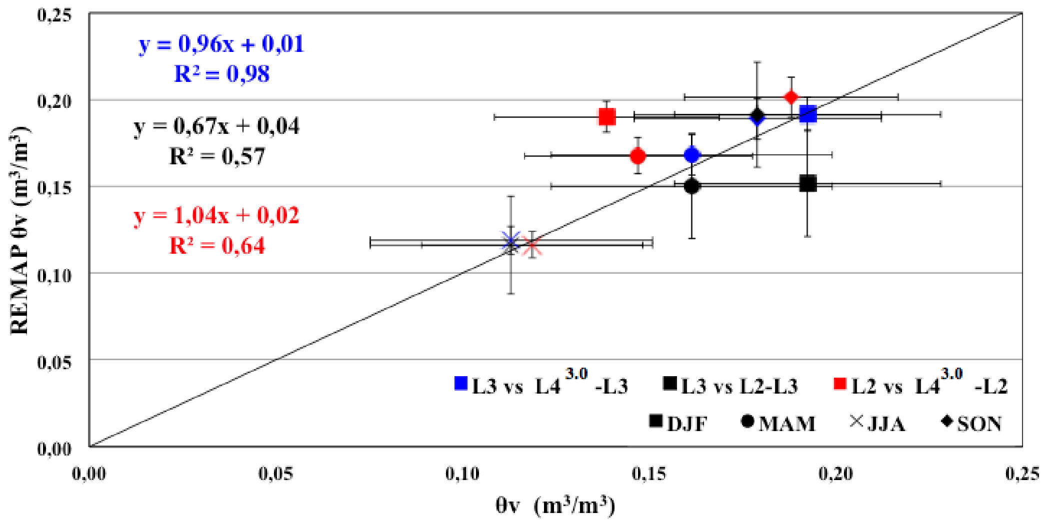

Figure 3: SMOS-derived SSM products comparison from different operational levels over the Iberian Peninsula.

(a)

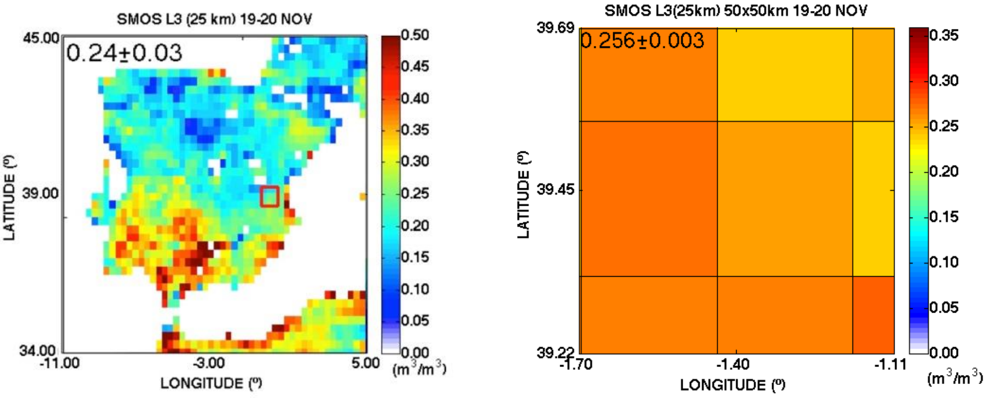

SMOS L3 (25 km) 19-20 NOV
0.24±0.03
LATITUDE (º)
LONGITUDE (º)
(m³/m³)
SMOS L3(25km) 50x50km 19-20 NOV
0.256±0.003
LATITUDE (º)
LONGITUDE (º)
(m³/m³)

(b)

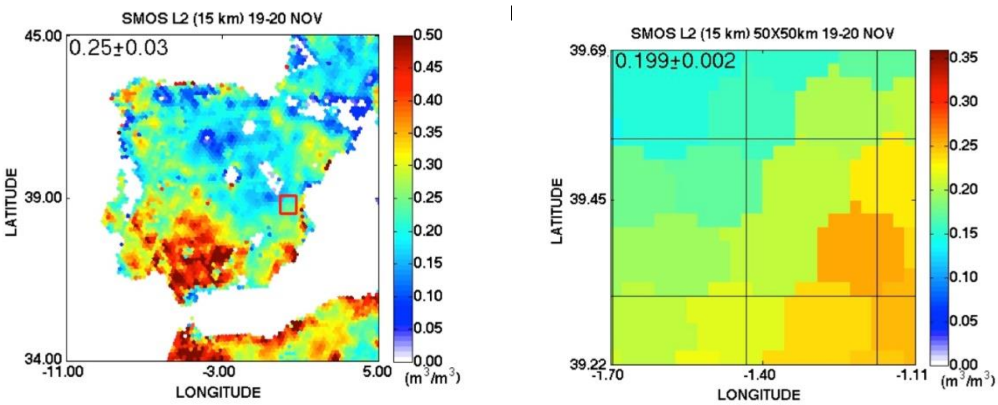

SMOS L2 (15 km) 19-20 NOV
0.25±0.03
LATITUDE
LONGITUDE
(m³/m³)
SMOS L2 (15 km) 50X50km 19-20 NOV
0.199±0.002
LATITUDE
LONGITUDE
(m³/m³)

(c)

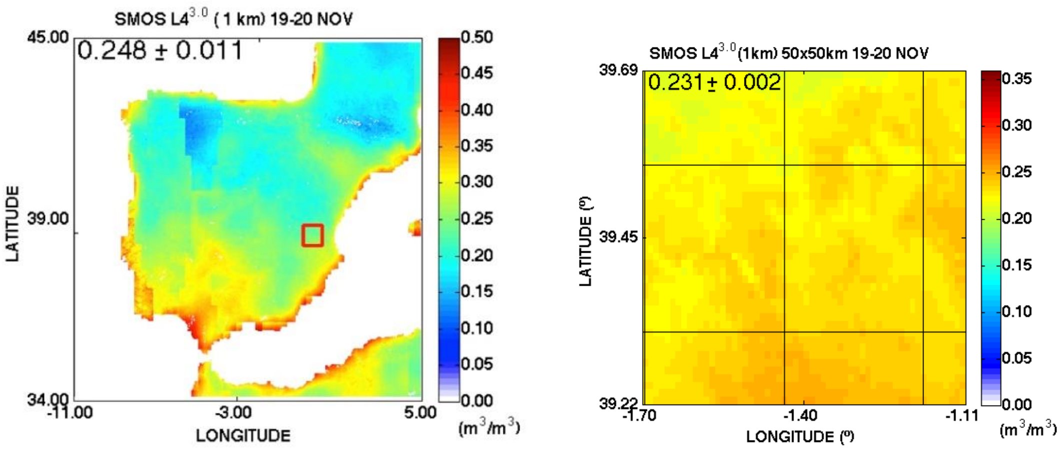

SMOS L4^3.0 (1 km) 19-20 NOV
0.248 ± 0.011
LATITUDE
LONGITUDE
(m³/m³)
SMOS L4^3.0(1km) 50x50km 19-20 NOV
0.231± 0.002
LATITUDE (º)
LONGITUDE (º)
(m³/m³)

Figure 4: Spatial distribution of SMOS-derived soil moisture (merged product: ascending and descending orbits are considered) over the Iberian Peninsula (left) and the VAS (right) as a mean for the 19-20 November of 2012 (a) SMOS-L3 (~25 km), (b) SMOS-L2 (~15 km), (c) SMOS-L4$^{\mathbf{3.0}}$ (~1 km). White empty pixels in (a) and (b) are indicative of a lack of data. Please be aware of the different colour scale used for the IP and VAS.

(a)

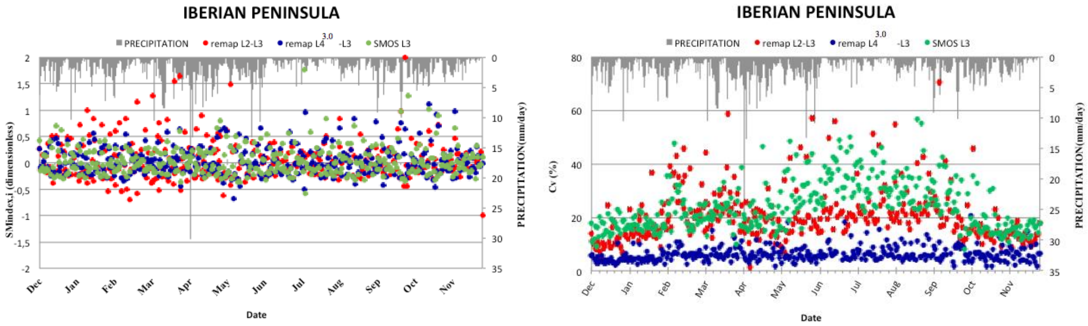

(b)

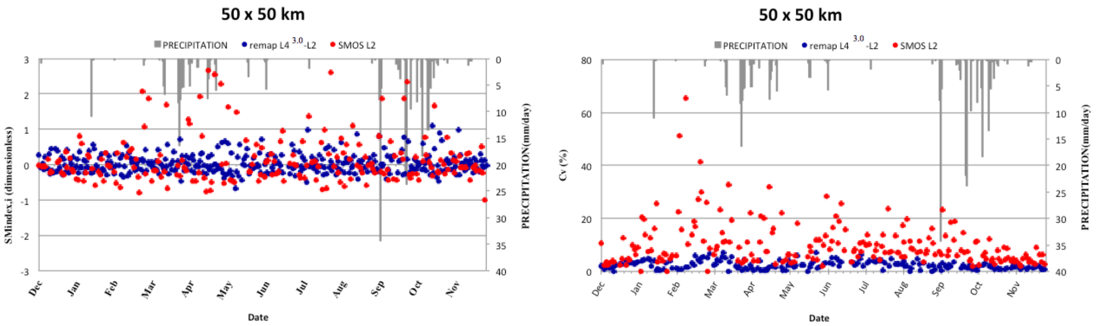

(c)

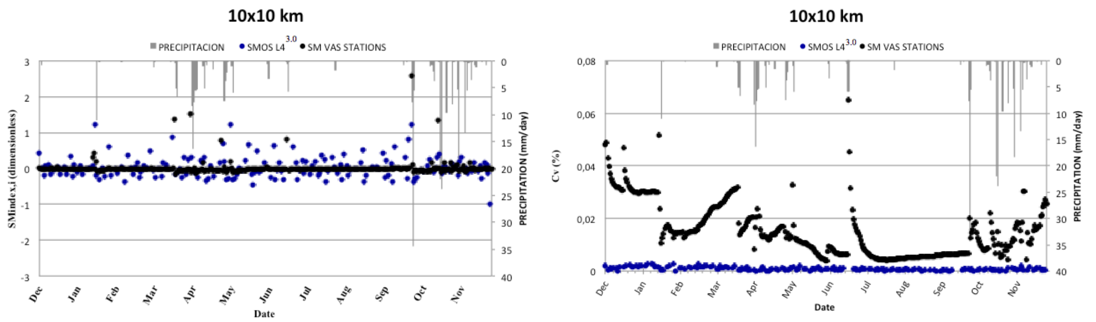

Figure 5: Averaged SMOS products and averaged ground-based observations of soil moisture evolution over the Iberian Peninsula (IP; top), the VAS area (centre), and the OBS area (bottom). Descending orbits are used. Precipitation from AEMET rain gauges on top. Left) Soil moisture daily index ($\Theta_{v\ index,i}$; dimensionless) and right) Coefficient of variation (Cv, %).

(a)

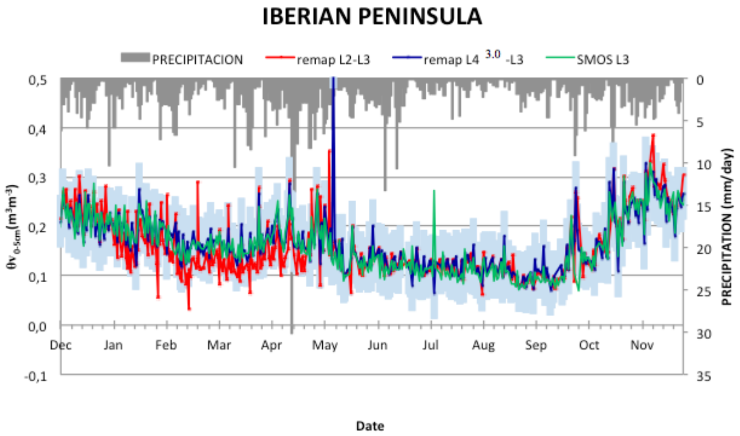

(b)

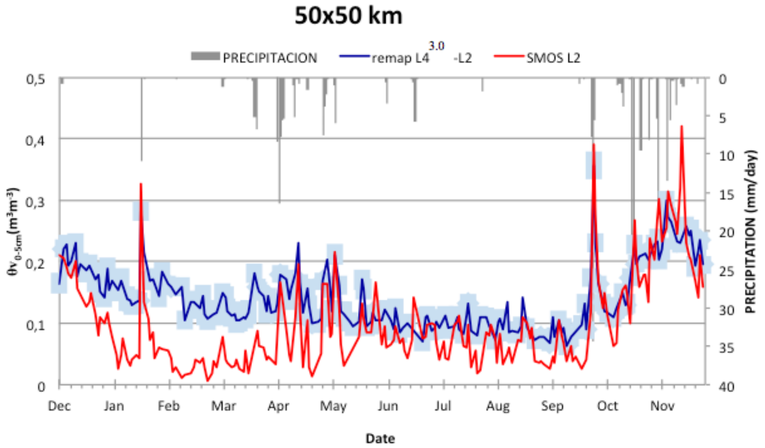

(c)

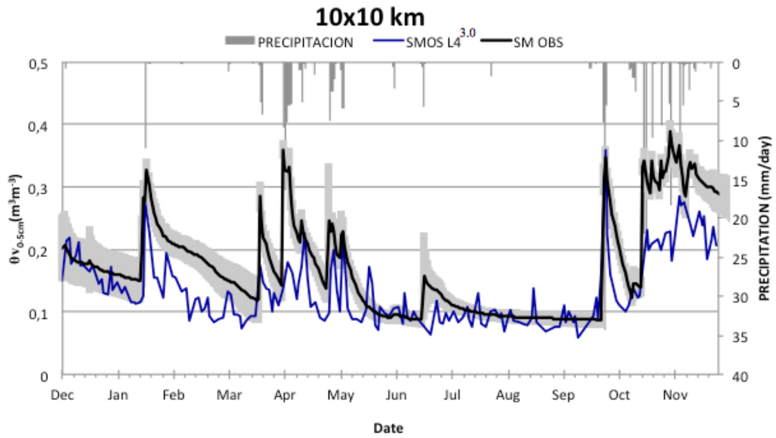

Figure 6: Temporal evolution of surface soil moisture time series averaged over the Iberian Peninsula (top), the VAS area (50 x 50 km^2; centre) and the OBS area (10 x 10 km^2; bottom). SMOS afternoon orbits are considered. Daily mean precipitation from the AEMET stations is shown on top of each plot. SMOS and remapped SMOS products are indicated in the plots. Shaded areas show standard deviations, respectively.

(a)

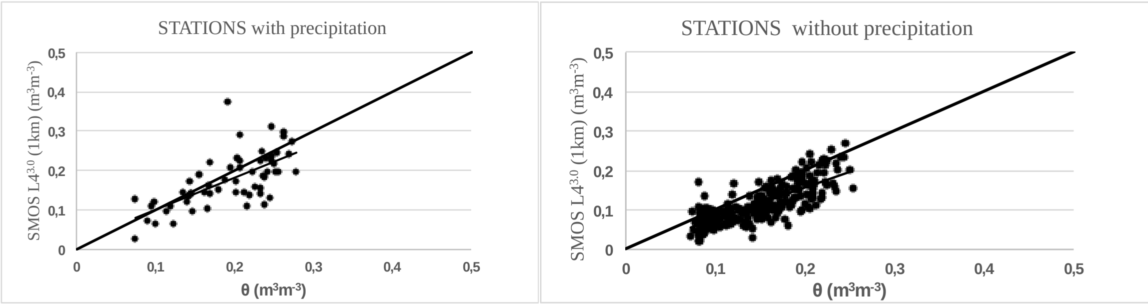

(b)

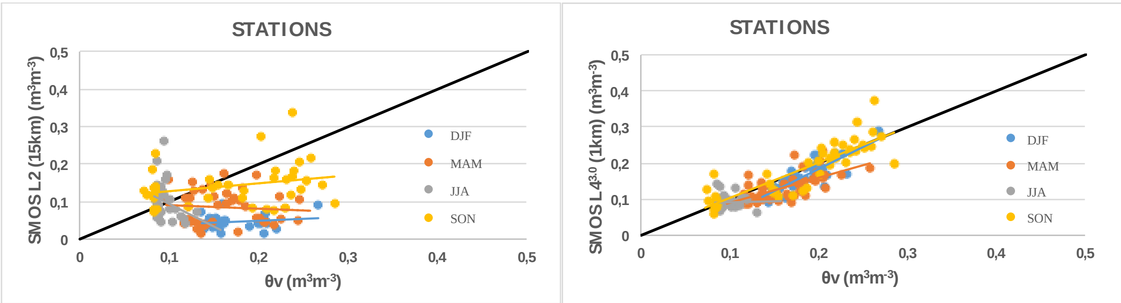

(c)

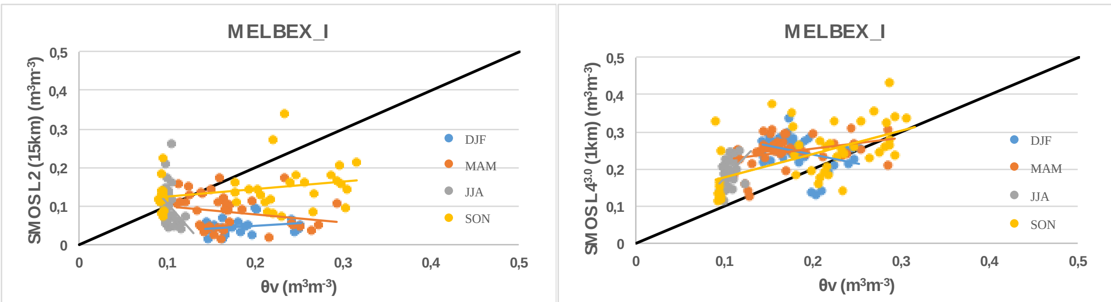

Figure 7: Results of the seasonal analysis for the hydrological year starting in December 2011. Scatter plots of (a) SMOS-L4$^{3.0}$ SSM (ascending and descending orbits) versus averaged 10x10 km^2 in situ soil moisture measurements (left) for days with precipitation, and (right) and without precipitation (< 1 mm /d). (b) SMOS-L2 and SMOS-L4$^{3.0}$ SSM (descending orbits) versus averaged 10x10 km^2 in situ soil moisture measurements. (c) SMOS-L2 and SMOS-L4$^{3.0}$ SSM (descending orbits) versus point-like ground measurements from MELBEX_I station, using the closest grid point. Segments are linear fit of seasonal data (3 months data). Statistics for individual comparisons at all stations are summarized in Table 3.

(a)

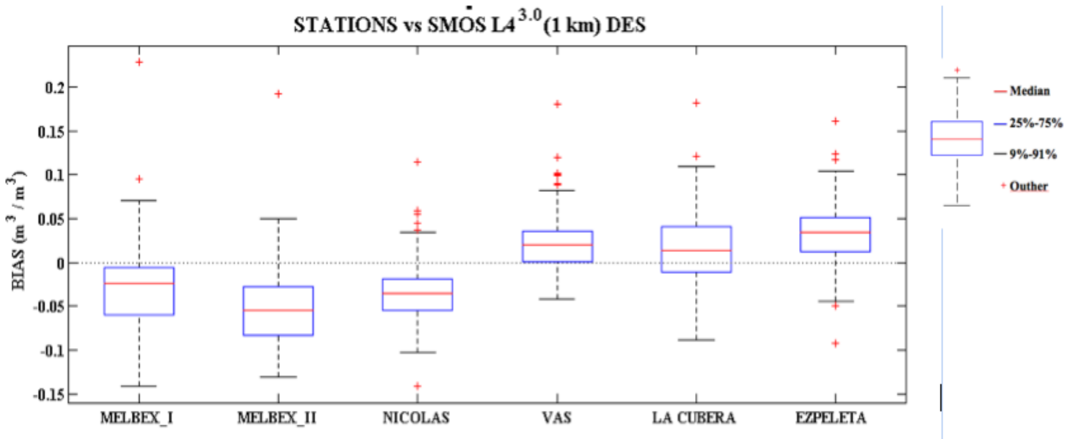

(b)

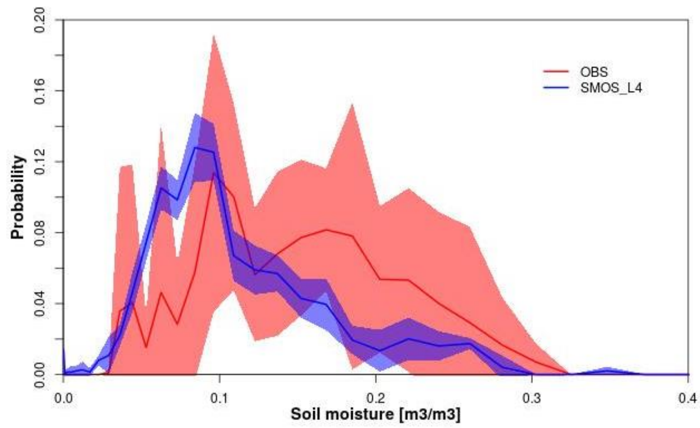

Figure 8: (a) Box plot of the comparison between point-like ground measurements at all stations over the VAS area and closest SMOS-L4$^{3.0}$ SSM data. (b) Probability distribution funtion (PDF) of SSM from in situ observations and SMOS- L4$^{3.0}$ SSM measurements. The standard deviations are indicated with shaded areas. Full lines represent the mean over all ground stations and over the 10 x 10 km^2 of the OBS area in VAS where the in SSM network is located.

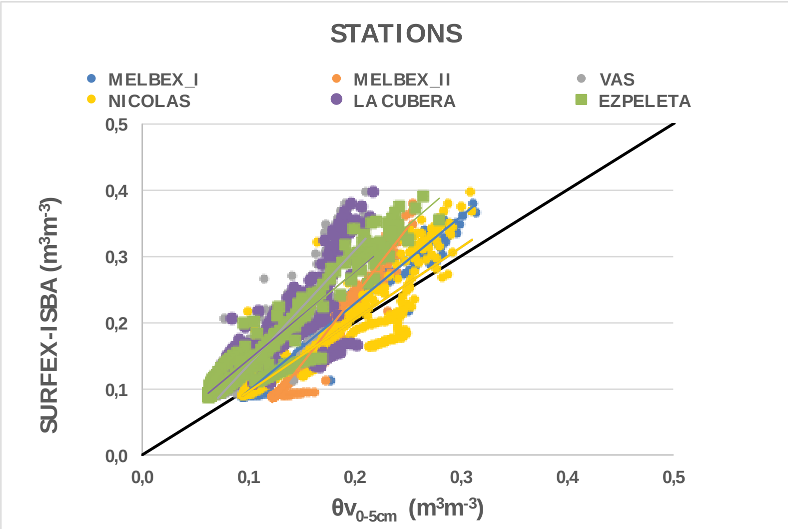

Figure 9: Scatter plot of temporal mean (over the whole simulation period) SSM ground measurements versus SURFEX(ISBA) simulations (realistic initial scenario; REAL-I) at all stations. Statistics for all stations using the REAL-I initial scenario are presented in Table 4.

(a)

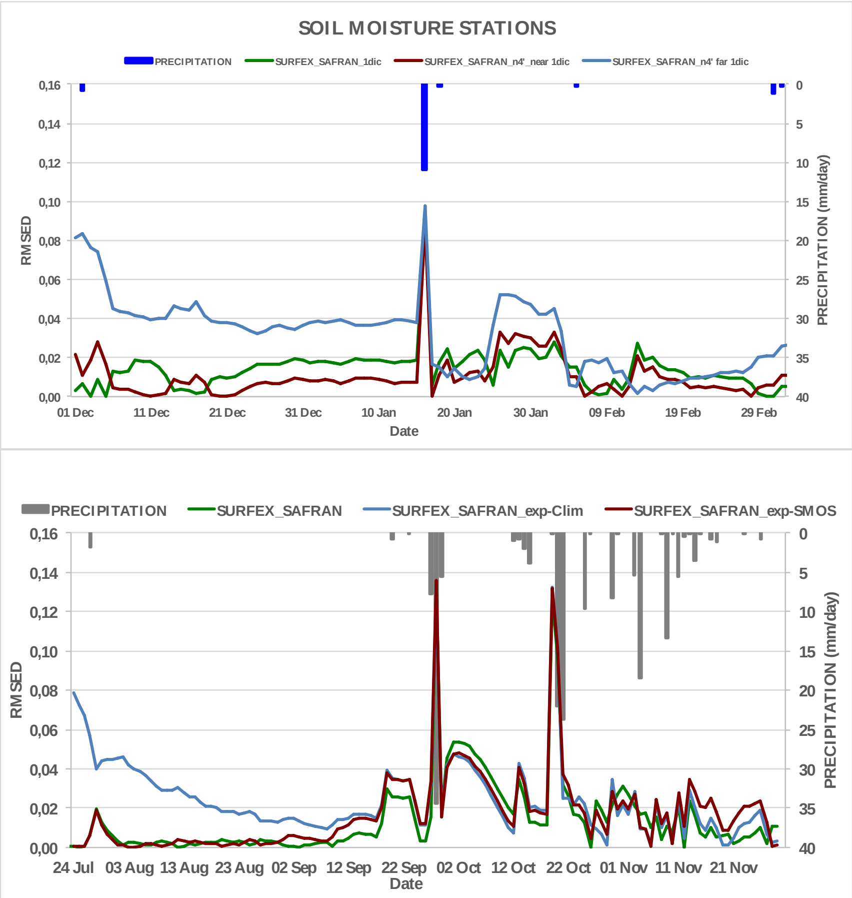
SOIL MOISTURE STATIONS
PRECIPITATION
SURFEX_SAFRAN_1dic
SURFEX_SAFRAN_n4'_near 1dic
SURFEX_SAFRAN_n4' far 1dic
RMSED
PRECIPITATION (mm/day)
01 Dec
11 Dec
21 Dec
31 Dec
10 Jan
20 Jan
30 Jan
09 Feb
19 Feb
29 Feb
Date
PRECIPITATION
SURFEX_SAFRAN
SURFEX_SAFRAN_exp-Clim
SURFEX_SAFRAN_exp-SMOS
RMSED
PRECIPITATION (mm/day)
24 Jul
03 Aug
13 Aug
23 Aug
02 Sep
12 Sep
22 Sep
02 Oct
12 Oct
22 Oct
01 Nov
11 Nov
21 Nov
Date

(b)

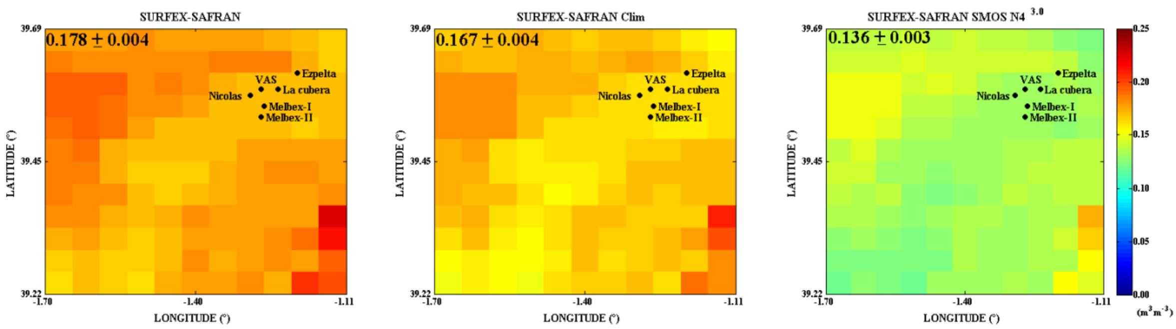
SURFEX-SAFRAN
0.178 ± 0.004
SURFEX-SAFRAN Clim
0.167 ± 0.004
SURFEX-SAFRAN SMOS N4 3.0
0.136 ± 0.003
VAS
Ezpelta
La cubera
Nicolas
Melbex-I
Melbex-II
LATITUDE (°)
LONGITUDE (°)
39.69
39.45
39.22
-1.70
-1.40
-1.11
0.25
0.20
0.15
0.10
0.05
0.00
(m³m⁻³)

(c)

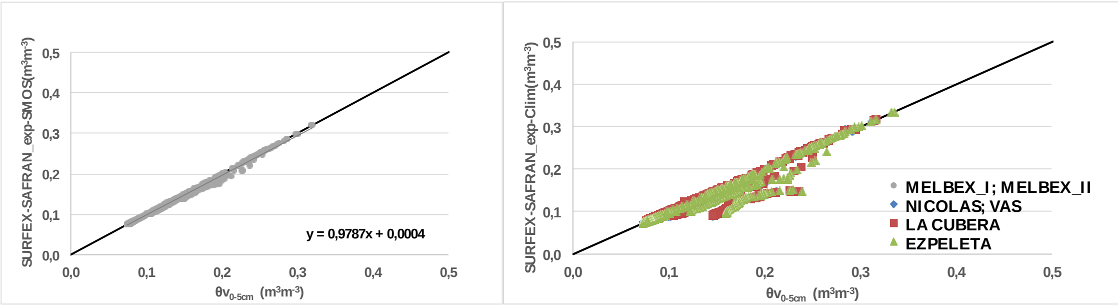

Figure 10: (a) RMSD for the daily mean SSM from the three SURFEX(ISBA) simulations with perturbed initial SSM scenarious (details in section 4.3.2). (b) Spatial distribution of mean SSM for the winter simulation (a, left) for the 3 simulations. (c) Scatter plot depicting the compariosn between in situ SSM observations and SURFEX-SAFRAN-SMOSL4$^{3.0}$ simulations, as a mean over all stations (left) and for each of the stations (right).